

AN ABSTRACT OF THE THESIS OF

Scott C. Franz for the degree of Doctor of Philosophy in Nuclear Engineering presented on May 6, 1997. Title: A Study of Return to Saturation Oscillations in the OSU APEX Thermal Hydraulic Testing Facility.

Redacted for Privacy

Abstract approved: _____



Jose N. Reyes, Jr.

The purpose of this paper is to describe the flow oscillations which occur in the AP600 long term cooling test facility at Oregon State University. The AP600 system is an advanced pressurized water reactor design utilizing passive emergency cooling systems.

A few hours after the initiation of a cold leg break, the passive cooling systems inject gravity fed cold water at a rate allowing steam production in the reactor vessel. Steam production in the core causes the pressure in the upper head to increase leading to flow oscillations in all the connecting reactor systems.

This paper will show that the oscillations have a definite region of onset and termination for specific conditions in the APEX testing facility. Tests performed at high powers, high elevation breaks, and small break sizes do not exhibit oscillations.

The APOS (Advanced Plant Oscillation Simulator) computer code has been developed using a quasi-steady state analysis for flows and a transient analysis for the core node energy balance. The pressure in the reactor head is calculated using a modified

perfect gas analysis. For tank liquid inventories, a simple conservation of mass analysis is used to estimate the tank elevations. Simulation logic gleaned from APEX data and photographic evidence have been incorporated into the code to predict termination of the oscillations.

Areas which would make the work more complete include a better understanding of two-phase fluid behavior for a top offtake on a pipe, more instrumentation in the core region of the APEX testing facility, and a clearer understanding of fluid conditions in the reactor barrel.

Scaling of the oscillations onset and pressure amplitude are relatively straight forward, but termination and period are difficult to scale to the full AP600 plant. Differences in the core power profile and other geometrical differences between the testing facility and the actual plant make the scaling of this phenomenon to the actual plant conditions very difficult.

©Copyright by Scott C. Franz
May 6, 1997
All Rights Reserved

A Study of Return to Saturation Oscillations in the OSU APEX Thermal Hydraulic
Testing Facility

by

Scott C. Franz

A THESIS

submitted to

Oregon State University

in partial fulfillment of
the requirements for the
degree of

Doctor of Philosophy

Completed May 6, 1997
Commencement June, 1997

Doctor of Philosophy of Scott C. Franz presented on May 6, 1997

APPROVED:

Redacted for Privacy

Major Professor, representing Nuclear Engineering

Redacted for Privacy

Chair of Department, representing Nuclear Engineering

Redacted for Privacy

Dean of Graduate School

I understand that my thesis will become part of the permanent collection of Oregon State University libraries. My signature below authorizes release of my thesis to any reader upon request.

Redacted for Privacy

Scott C. Franz, Author

Acknowledgment

I would like to acknowledge the help of many people who made this work possible. First and foremost, I would like to thank my wife Wendy who has supported me through many trying times during the course of my graduate career. Wendy has made a six year sacrifice to stand beside enduring a lot of changing deadlines and me not having a paying job. Next I would like to thank Dr. Jose Reyes who has been my mentor, my friend, my brother and my confidant. His expert opinion and well trained background has helped me through those crazy little things I couldn't see but he could see so well. When Jose and I are working together, I am reminded of the scripture, "As steel sharpens steel, so one man sharpens another."

I would also like to thank the APEX facility team for their support and the friendship I have received from them over the years. The project has been a great success and I am proud to have had the opportunity to be involved with them and the project.

Finally, I want to thank God for giving me everything I have found here at OSU. The blessings he has provided me have been tangible and intangible but all things I have were given to me through Christ.

TABLE OF CONTENTS

	<u>Page</u>
1. A Study of Return to Saturation Oscillations in the OSU APEX Thermal Hydraulic Testing Facility.....	1
1.1 Introduction and Research Objectives.....	1
1.2 The AP600 Test Facility.....	3
1.2.1 Core Makeup Tanks (CMT's).....	5
1.2.2 Incontainment Refueling Water Storage Tank (IRWST).....	6
1.2.3 Sumps (Primary and Secondary).....	6
1.2.4 Accumulators (ACC's).....	7
1.2.5 Automatic Depressurization Systems (ADS).....	7
1.2.6 Primary Residual Heat Removal Heat Exchanger (PRHR).....	8
2. Previous Work on Fluid Oscillation Behavior.....	9
2.1 Overview.....	9
3. Return to Saturation Oscillations.....	12
3.1 Introduction to the Oscillations.....	12
3.2 What Are the Return to Saturation Oscillations?.....	12
3.3 What does the RSO Look Like?.....	16
3.4 What are the Potential Mechanisms?.....	16
3.4.1 Increased Steam Venting due to Changing Core Exit Quality.....	17
3.4.2 Changing Momentum in Exit Flow.....	18
3.4.3 Condensation in the Downcomer.....	22
3.4.4 Pressure Oscillation in the Sump.....	24
4. Description of RSO Mechanisms.....	26
4.1 Introduction.....	26
4.2 Pre RSO.....	28
4.3 Stage One.....	29

TABLE OF CONTENTS (Continued)

	<u>Page</u>
4.4 Stage Two	29
4.5 Stage three.....	29
4.6 Stage Four	29
4.7 Termination.....	31
5. Oscillation Characteristics.....	32
5.1 Introduction.....	32
5.2 Onset	32
5.3 Termination.....	32
5.4 Period	35
5.5 Amplitude	36
5.6 Recirculation patterns in the barrel.....	36
6. Numerical Analysis of the Oscillations (APOS Code).....	39
6.1 Introduction.....	39
6.2 General Descriptions of the APOS Code.....	39
6.3 APOS Code General Assumptions	40
6.3.1 Injection and Exit Flows.....	40
6.3.2 Core Temperature Profile.....	40
6.3.3 The Perfect Gas Assumption.....	41
6.4 Governing Equations of the APOS Code	41
6.4.1 Node 1, IRWST Equations.....	42
6.4.2 Node 2, DVI Line Equations.....	44
6.4.3 Node 3, Downcomer Below DVI and Reactor Lower Vessel Plenum.....	49

TABLE OF CONTENTS (Continued)

	<u>Page</u>
6.4.4 Node 4, The Nodalized Core (20 core nodes)	50
6.4.4.1 Core Nodes at Subcooled Conditions.....	51
6.4.4.2 Core Nodes at Saturated Conditions	54
6.4.5 Node 5, Steam Volumes	56
6.4.6 Node 6, Upper Plenum, Upper Downcomer.	59
6.4.7 Node 7, ADS 4 Line	61
6.5 Onset and Termination	67
7. Comparisons of the APOS code with APEX plant data.....	72
7.1 Introduction.....	72
7.2 The NRC-13 test series	72
7.3 NRC Data Comparisons	76
7.4 Conclusions.....	80
8. Scaling to the actual AP600	81
8.1 Introduction.....	81
8.2 Oscillation characteristics which can be scaled.....	81
8.3 Oscillation characteristics which make scaling very difficult	82
9. Conclusions and Summary	83
9.1 General Overview	83
9.2 Safety and Scaling Issues.....	85
9.3 Roadmap for future work.....	86
Bibliography.....	88
Appendix APOS Code Listing	90

TABLE OF CONTENTS (Continued)

	<u>Page</u>
Nomenclature and Subscripts.....	97

LIST OF FIGURES

<u>Figure</u>		<u>Page</u>
1.1	General 3D picture showing the general layout of the AP600 design.....	2
1.2	Line Drawing of the APEX testing facility main piping layout.....	5
3.1	APEX data showing ADS4 liquid flow during RSO.	13
3.2	APEX data showing DVI flow during RSO.....	13
3.3	APEX data showing break flow during RSO.....	14
3.4	APEX data showing RX pressure during RSO.	14
3.5	APEX data showing reactor liquid levels during RSO.	15
3.6	APEX data showing core fluid temperatures during RSO.....	15
3.7	Figure showing the comparison between simulated pressure oscillations and ADS4 liquid flow oscillations. Notice how well the ADS4 flow follows the pressure.....	20
3.8	Figure showing the time lag between reactor simulated pressure and ADS4 flow for a fictitious ADS4 pipe length.	21
3.9	Momentum distortion for an extreme fictitious ADS4 pipe length and liquid mass.....	22
3.10	The energy percentage contributions for the RSO.....	23
3.11	Total energy out of the primary system during the RSO.....	24
3.12	Pressure in the reactor head and primary sump during RSO.....	25
4.1	APEX system before oscillation onset.....	27
4.2	Stage 1 and 2. View of the APEX test facility when the oscillations begin. The ADS4 line is sealed with some standing water in the ADS4 line.....	28
4.3	Stages 3 and 4. This figure shows the liquid inventory conditions for the plant at the point when ADS4 begins to flow with a two-phase mixture.	30
4.4	Oscillation termination.....	31

LIST OF FIGURES (Continued)

<u>Figure</u>		<u>Page</u>
5.1	Plot showing onset and termination with APEX oscillation data for test NRC-5013.	34
5.2	Plot showing onset and termination with APEX oscillation data for test NRC-6213.	35
5.3	APEX data showing steam exiting the reactor through the break and ADS4 lines during RSO.	37
5.4	APEX data showing the temperature depression in the center of the reactor core.	38
6.1	Components of the RSO.....	42
6.2	Plot showing the quality versus ADS4 liquid flow.	64
6.3	Flow chart for the APOS code. Dashed Lines indicate sections of the code which represent changing reactor inputs.....	66
7.1	Plot showing the three RSO onsets for the NRC-6113 test.....	74
7.2	Photo showing the ADS4 piping during the RSO.....	75
7.3	Plot showing APOS code results to actual APEX data for pressure.	76
7.4	Plot showing APOS code results to actual APEX data for IRWST Level.	77
7.5	Plot showing APOS code results to actual APEX data for core power.....	77
7.6	Plot showing APOS code results to actual APEX data for DVI Flow.	78
7.7	Plot showing APOS code results to actual APEX data for core temperatures.	79
7.8	Plot showing APOS code results to actual APEX data for the RX mean free surface.	79
7.9	Plot showing APOS code results to actual APEX data for ADS4 liquid flows.	80

1. A Study of Return to Saturation Oscillations in the OSU APEX Thermal Hydraulic Testing Facility

1.1 Introduction and Research Objectives

The safety of a nuclear reactor is of interest to many people. This general concern for nuclear plant safety has motivated designers to develop innovative ways to safely protect the fuel in nuclear power plants. A new design on the horizon is the Westinghouse AP600 or Advanced Passive 600 megawatt plant (1). This new design as shown in Figure 1.1, has several new safety features which require testing to insure the adequacy of their performance.

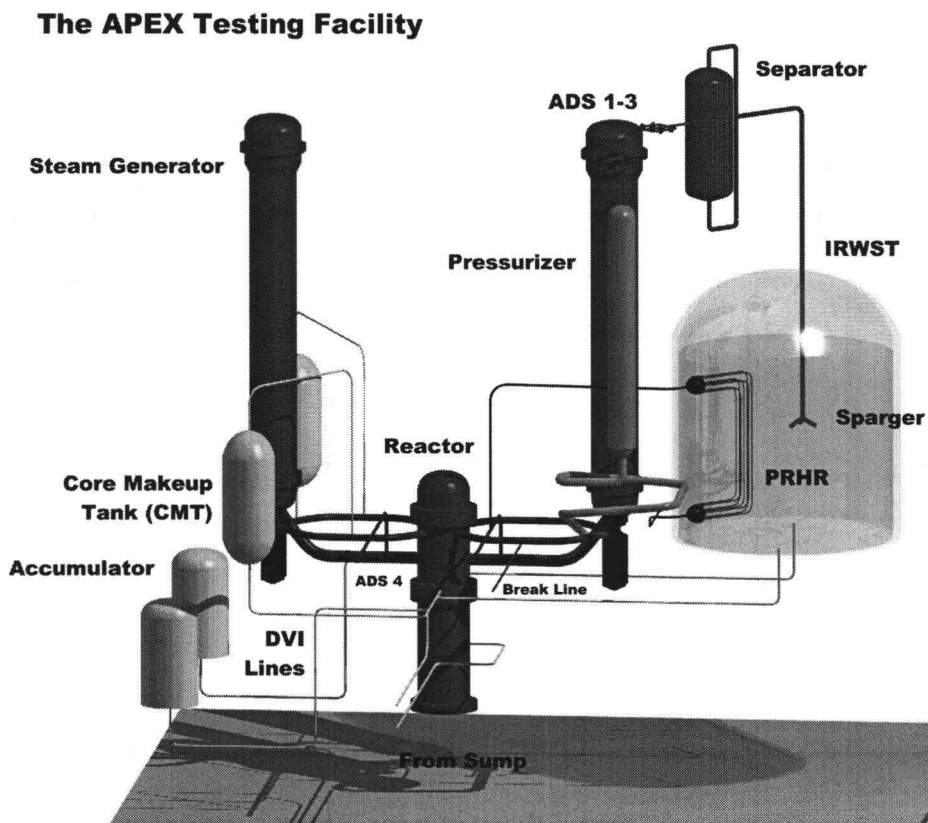


Figure 1.1 General 3D picture showing the general layout of the AP600 design.

Westinghouse has built a 1/4 scale model of the AP600 design at Oregon State University (2). This testing facility is called APEX or Advanced Plant EXperiment. The facility models all of the safety systems of the actual design. The experiments at the facility simulate a variety of plant failures with the goal of studying the safety systems performance. During the testing of the AP600 design, several types of pressure oscillations in the reactor vessel were observed late in the cold leg break transients. One particular set of oscillations occurred when the fluid at the core exit returned to a saturated condition after being subcooled. These oscillations are the focus of this paper.

The objective of this research was to understand the mechanisms which governed the behavior of this particular phenomenon, construct a computer code to simulate these oscillations, and to determine the possible implications of the phenomenon to the full scale power plant.

Chapter two is a description of oscillations in steam water systems. Chapter three is an overview of the oscillations this paper covers in particular.

Chapter four describes the development of a set of oscillations during a cold leg break scenario. Six stages of the oscillations are described. The first stage includes the plant conditions required to produce oscillations followed by the four stages during oscillations and the sixth stage describes oscillation termination. Chapter five describes five particular characteristics of the oscillations which are onset, termination, period, amplitude, and the impact of core fluid recirculation patterns on oscillation behavior. Chapter six is a description of the APOS model and chapter seven provides comparisons of model predictions to actual APEX data. Chapter eight is a discussion of oscillation scaling issues.

The rest of this introduction will cover most of the safety systems employed in the design. Later chapters will cover how these safety systems interact to cause the oscillations of interest.

1.2 The AP600 Test Facility

The AP600 Test facility was constructed to test a prototype nuclear reactor design by Westinghouse (1). The new design is titled AP600 (for Advanced Passive 600 megawatt plant). The motivation behind the testing was to determine the behavior

of several new safety systems inherent to the new design. Several key features of these new safety systems are the passive nature of the design and the simplicity of actuation, construction and maintenance.

A passive safety system employs gravity as a driving mechanism for fluid flow rather than an active pump driven system. In order for cool safety injection water to flow by gravity into a highly pressurized system, the source of the safety injection water must be at the same pressure as the system it is intended to protect. The AP600 design achieves this goal by using pressure balance lines between the primary reactor cooling loop and the tanks holding the safety injection water. Hot steam and lighter more buoyant hot liquid can flow up into the balance line while cool heavier safety water flows into the primary system. This design philosophy is very beneficial due to the lack of mechanical pumps, wiring, actuation mechanisms, and other support systems needed to perform active injection. Expense of construction, design, and maintenance is greatly reduced. Another great advantage using gravity is the tremendous reliability it provides.

The Safety systems of AP600 include several tanks in the facility. All of the safety injection water passes through two special pipelines called the Direct Vessel Injection lines (or DVI lines). These injection lines are connected to the tanks described below and directly to the vessel near the hot leg elevation. The water flowing through this line passes into the reactor downcomer allowing water to flow to the core and flood the reactor during a transient. The following is a brief description of each of these tanks and their role in the safety of the AP600 design. Figure 1.2 shows the basic pipe layout for the APEX testing facility.

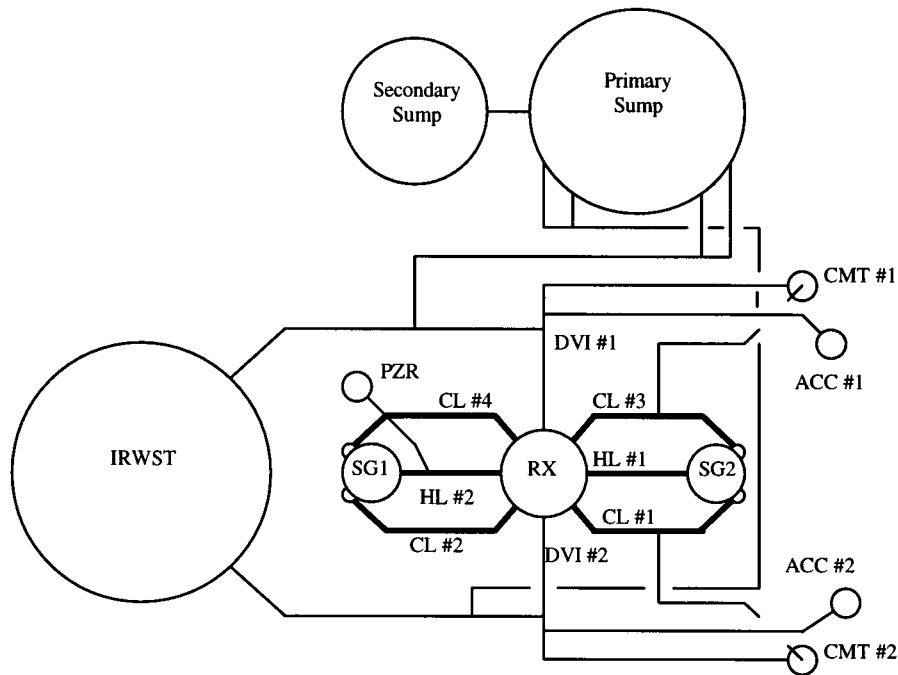


Figure 1.2 Line Drawing of the APEX testing facility main piping layout.

1.2.1 Core Makeup Tanks (CMT's)

The core makeup tanks in the AP600 design are used for cold water injection during a transient. The CMT's are held at the same pressure as the primary system with the use of a pressure balance line with connections from the primary cold legs to the tops of the tanks.

Because the tanks are kept at the same pressure as the primary system and the elevation of the tanks is above the reactor, water can drain into the primary with the use of gravity only. A gravity fed system makes this attractive as a safety system requiring no pumps and very few valves.

1.2.2 Incontainment Refueling Water Storage Tank (IRWST)

The IRWST is a large tank in the AP600 design used primarily as a source of water during reactor refueling. The water in the tank is used to flood the deck above the reactor in order to provide cooling to the fuel and shielding to the containment building when fuel assemblies are moved around.

The tank is also used as an automatic depressurization system during a transient. Both the PRHR (Primary Residual Heat Removal) heat exchanger and the first three ADS (Automatic Depressurization System) trains dump heat into the IRWST by natural convection and by purging hot water and steam directly into the tank. The water is also used as a reservoir of cold injection water which drains by gravity when the pressure in the primary system is low (approximately atmospheric pressure).

1.2.3 Sumps (Primary and Secondary)

In reactor designs, the containment building has a large air space below the reactor to catch any water during a transient. This large volume is called the sump and typically has a curb surrounding the volume.

When the sump fills, the water overflows the curb and begins to fill the lower containment compartment sump. In the APEX test facility, these sumps are simulated using two large tanks connected with a pipe at the proper elevation.

1.2.4 Accumulators (ACC's)

The AP600 design employs two small tanks which inject cold water at a pressure between operating and atmospheric pressures. These tanks inject their water using a pressurized bubble of Nitrogen at the top of the tank. A check valve in the injection line keeps high pressure primary water from entering the accumulator. When the primary pressure drops below the pressure in the tank, the check valve opens and the water in the tank flows into the primary system.

This Nitrogen bubble gas eventually flows into the DVI line after the liquid has been purged from the tank. The AP600 system has 10 bypass holes in the top of the downcomer to allow Nitrogen gas to flow from the downcomer into the upper head of the reactor vessel.

1.2.5 Automatic Depressurization Systems (ADS)

The automatic depressurization system is used to quickly bring the primary plant from operating pressure down to atmospheric pressure in a controlled manner. It is advantageous to reduce the primary pressure in a reactor system during a transient. Lower primary pressures aid powered injection systems to inject cool water and provides the accumulators and IRWST an opportunity to begin injection.

The ADS system in the AP600 design has four separate stages. The first three stages are actuated when the level of water in the CMT drops to specified levels. The first stage has a smaller flow area than the second and third stages. The sequential opening of the individual stages of the ADS train allows primary water and steam to

flow from the top of the pressurizer into a large sparger located in the IRWST. The energy of the hot water and steam is absorbed into the large volume of colder water in the IRWST allowing for a controlled primary system depressurization.

The fourth stage ADS begins on a low CMT liquid level. The fourth stage provides a path for primary water in the hot legs to vent to the sump.

1.2.6 Primary Residual Heat Removal Heat Exchanger (PRHR)

The PRHR is used to take heat given off by the core and transport it to the IRWST. This large heat exchanger is located inside the IRWST and has connections to the primary system cold leg and the steam generator channel head. Flow through this heat exchanger is driven by natural circulation.

2. Previous Work on Fluid Oscillation Behavior

2.1 Overview

The work performed for fluid systems concerning oscillation behavior fall under several categories. The oscillations of interest in this work have long periods (on the order of a minute to two minutes). For oscillations in systems where the periods are short (on the order of seconds or fractions of seconds), the phenomenon generally is caused by pressure gradients (shock waves) either through a rigid tube or pipe or by some type of back pressure subsonic communication through an orifice or other constriction (3,4).

There are roughly six different types of oscillations,

- Buoyancy wave
- Density-controlling instability
- Pressure wave due to compressible volume (Helmholtz wave)
- Thermal-excursion-coupled wave
- Acoustic wave
- Mechanical vibration

A specific category for an oscillation in similar systems is called a density-controlling instability. This oscillation occurs in a system where a flow restriction exists at the exit of a heated section. Liquid passing through the restriction slows down the flow of fluid through the heated section. When this occurs, the fluid in the heated section increases its void. When the two-phase fluid slug passes through the restriction,

the lighter, more voided, fluid flows through the restriction more rapid than the single-phase fluid slug. The increase in flow through the heated section then reduces the void and the cycle starts over.

This phenomenon is very similar to the RSO but the differences in communication between the heated section, the exit flow restriction and the void make the analysis approaches to this type of phenomenon unusable.

For the APEX oscillation phenomenon, no pressure gradients are observed in the injection or ADS4 lines. Constrictions in the lines introduce very small frictional head losses during the phenomenon of interest. Because of these reasons, the research in pressure wave and density wave analysis does not apply to the APEX oscillation phenomenon.

Another category for system oscillation behavior falls under a thermosiphon instability (3,5,6). A thermosiphon requires some type of natural circulation closed loop around a heat source and a heat sink. The buoyancy forces in the loop causes an instability which is tied to some type of void distribution. This system geometry does not apply to the RSO phenomenon.

Other oscillation phenomenon deal with systems which have some type of spring action. The spring acting component can be a gas volume attached to the piping, or sometimes the system has some flexible hose or conduit in the system which can swell and shrink with internal pressure differences (7,8). Long periods in these systems can be attributed to the time needed for the swelling or shrinking wave front to traverse the flexible conduit. Momentum plays a large role for a spring system. When studying the

equations which govern spring systems, the moving mass and spring constants govern the oscillation behaviors.

For this particular phenomenon, the mass in the system which is moving (primarily the liquid in the injection and ADS4 lines) is very small which rules out theories using spring momentum analysis.

Another type of oscillation concerns the boiling behavior in the heated region. If the fluid flow through the heated region is such that the temperature difference between the surface of the heater and the bulk fluid temperature oscillates around the critical temperature difference (i.e. the temperature leading to departure of nucleate boiling), the steam generation and void fraction can cause serious instabilities (3). Geyser phenomena falls into this kind of oscillation. This kind of behavior is not observed in the APEX facility.

There are naturally different types of oscillations concerning waves. At the point of RSO, the system configuration which could contribute oscillations due to waves is not large enough for a wave motion which is on the time order of the RSO (9).

In general, a large amount of work has been done on oscillations for forced convection systems. For the RSO, we are studying the system during a natural convection phase of the transient which is a region of study which is incomplete. Reading further ahead, it becomes obvious that the primary cause of these oscillations is due to an unstable gas venting mechanism in the hot leg. Information on the APEX oscillation mechanism is exceptionally sparse and therefore very little information can be gleaned from previous research.

3. Return to Saturation Oscillations

3.1 Introduction to the Oscillations

Pressure, level and flow oscillations in the Oregon State University APEX test facility have been observed for a small range of test conditions (10,11,12). The oscillations of interest to safety are pressure oscillations in the reactor head which directly affect the flow of injection water into and out of the reactor vessel. Therefore this work will focus on the set of oscillations which concern the interaction between the IRWST, the reactor, the ADS4, and the sump. This set of pressure, level and flow oscillations occurs after the reactor vessel fluid has become subcooled and returns to a saturated condition at the exit of the core. They are henceforth called, "Return to Saturation Oscillations," (RSO).

3.2 What Are the Return to Saturation Oscillations?

The interactive parameters surrounding the RSO in the APEX test facility have a common link, the pressure in the reactor head. These pressure oscillations directly affect the flow of water through the DVI line into the reactor vessel causing flow oscillations. Pressure oscillations also directly affect the flow of water out of the reactor through several different exits. The pressure oscillations of interest occur late in a transient which leaves two main paths for water (whether steam or liquid) to leave the primary system; the fourth stage ADS line and the simulated system break. Figures 3.1 through 3.6 show RSO oscillations in several of the APEX systems.

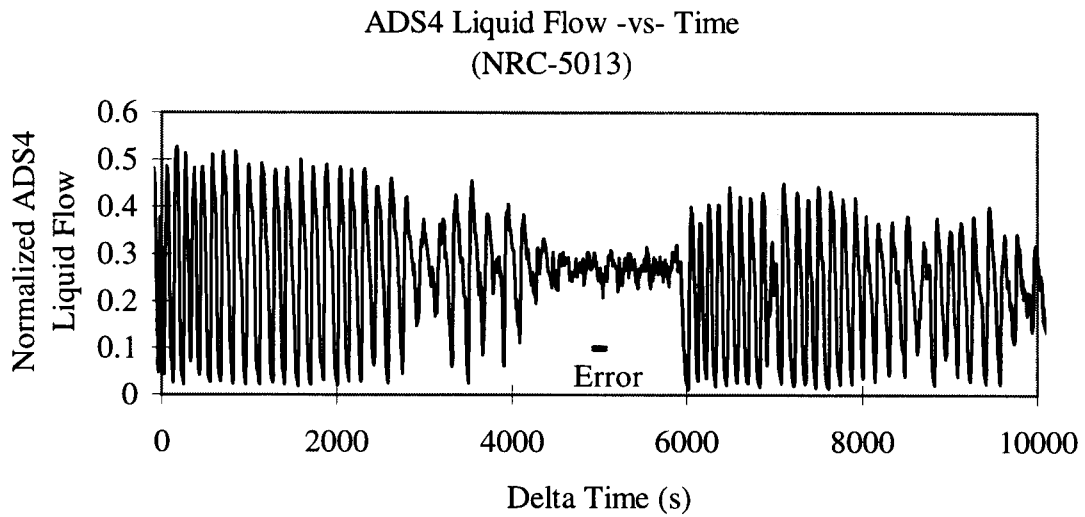


Figure 3.1 APEX data showing ADS4 liquid flow during RSO.

Figure 3.1 shows the oscillations produced during tests. Note the termination of the oscillations in the center of the plot. A detailed description of the NRC-13 test series is provided in section 7.2.

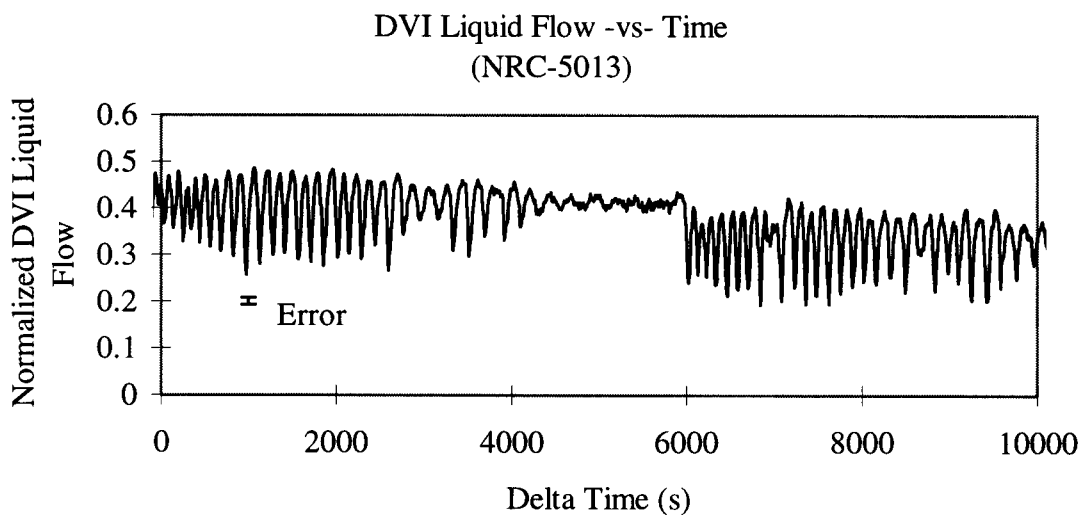


Figure 3.2 APEX data showing DVI flow during RSO.

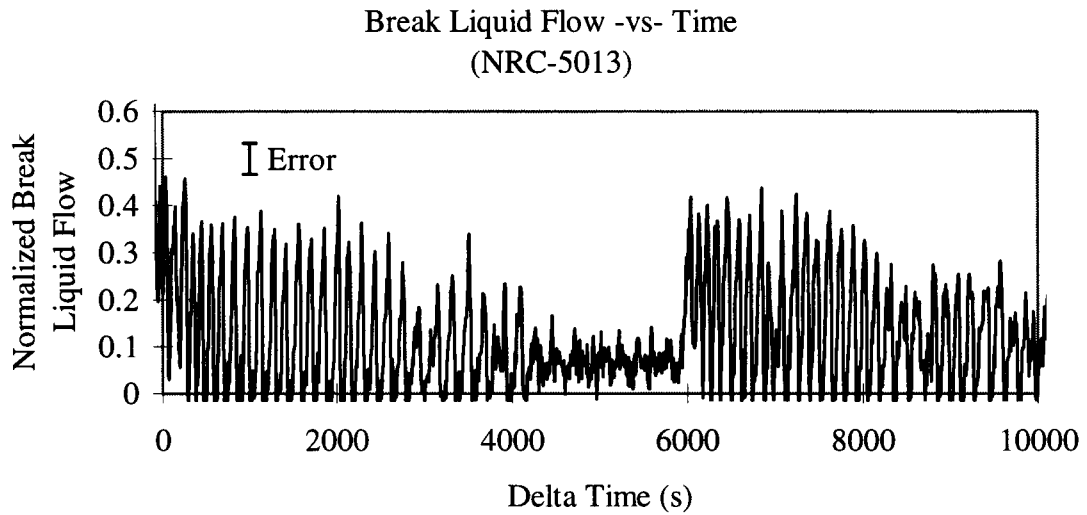


Figure 3.3 APEX data showing break flow during RSO.

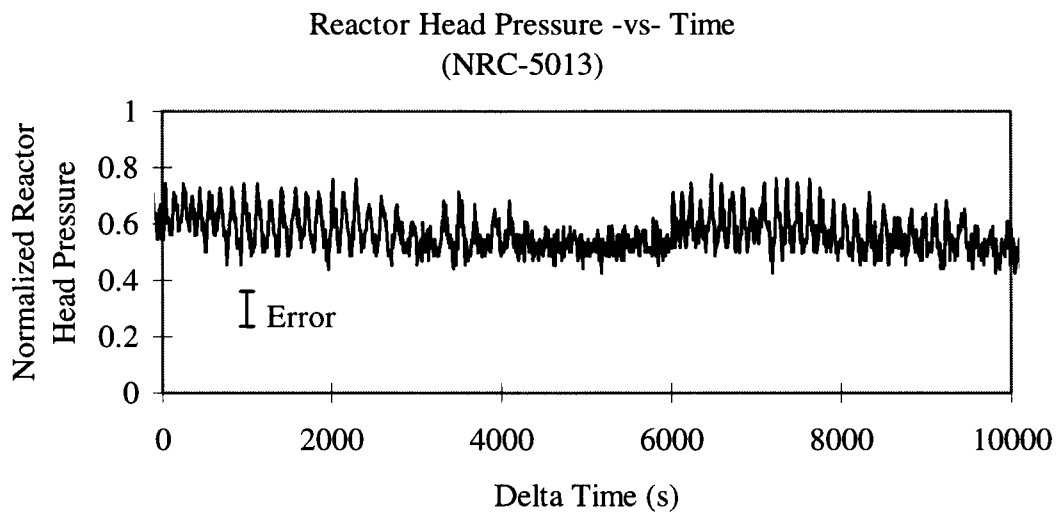


Figure 3.4 APEX data showing RX pressure during RSO.

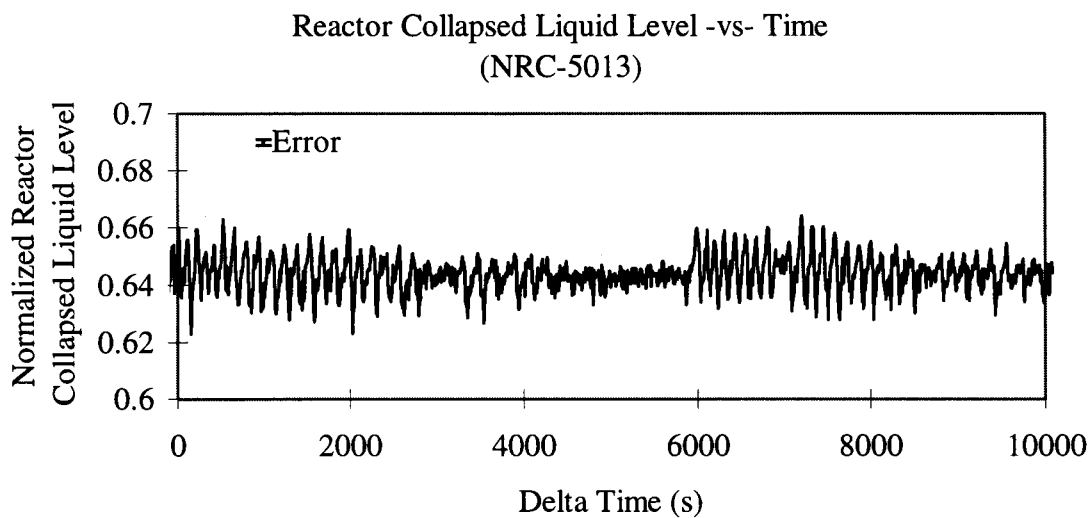


Figure 3.5 APEX data showing reactor liquid levels during RSO.

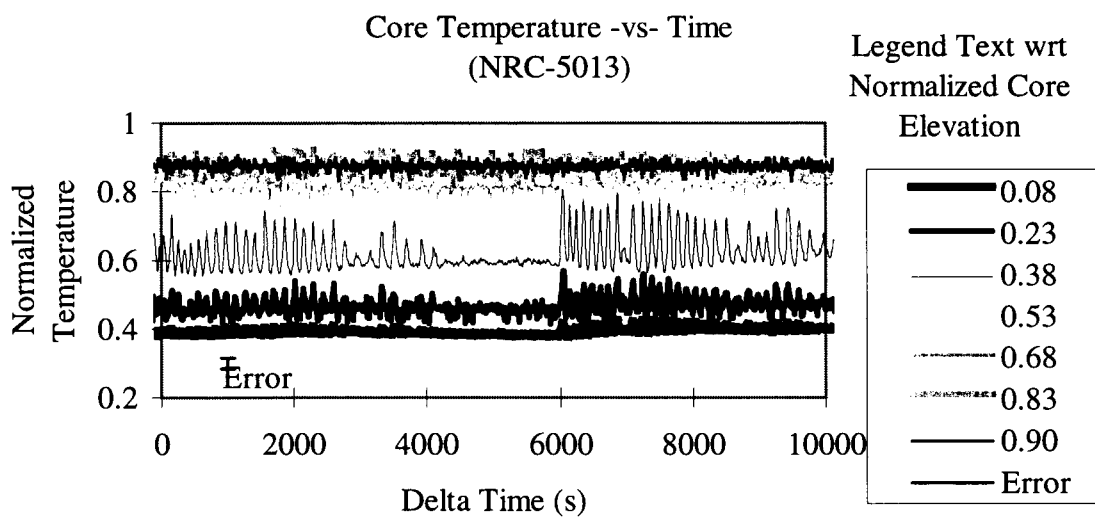


Figure 3.6 APEX data showing core fluid temperatures during RSO.

3.3 What does the RSO Look Like?

The RSO has two distinct shapes. One shape is typical of any wave, the waveform is that of a sine or cosine wave. A second shape of a wave has a hump or “ski slope” in it. Humps occur late in the RSO or when the system becomes destabilized and is nearing an oscillation termination point. Typical wave frequencies are on the order of a few minutes and have pressure amplitudes of 1 kPa or a few tenths of a psi. RSO durations have an average of about one hour.

3.4 What are the Potential Mechanisms?

The oscillations require the pressure in the reactor to change via an unstable mechanism. The reactor pressure is governed by a balance between steam production, steam venting, and condensation. The steam production mechanism is readily understood and is directly coupled to the safety injection flow rate, core power, break flow path, and break flow rate. Steam production in the core begins when liquid at the top of the core reaches saturation temperature. Injection water is heated as it passes through the core from the bottom to the top. The core exit temperature is therefore related to the time it takes for water to pass through the core and the core power. Flow rates through the core are related to the driving head of the injection system and the flow split of water to the core and potentially to the break.

When the flow of water through the core is sufficiently low enough to heat the water to saturation temperature, the liquid boils causing steam to fill the reactor head. If the flow rate through the core decreases, the liquid passing through the core acquires

more energy causing the overall steam generation rate to increase. If the flow rate through the core increases, the liquid passing through the core acquires less energy which decreases the steam production.

If the break in the system is in a cold leg, it is possible for some of the injection water to flow out of the break instead of passing through the core. This injection water flow split between the break and the core reduces the core inlet flow, inducing a higher steam production rate. This effect has been studied and is explained in section 5.4 and has been found to be almost always irrelevant. The data indicates the fluid through the break is mostly liquid with very little steam. However the amount of fluid exiting the break is not a strong contributing factor in the oscillations. The fluid exiting the break contributes to the period of the oscillation but the break does not need to exist for oscillations to occur. For several tests, the sump liquid level overwhelms the break elevation and liquid flows stop and sometimes flow back into the reactor through the break piping.

Pressure oscillations require the mechanism for steam removal to be unsteady. The following sections examine some possible steam consumption mechanisms.

3.4.1 Increased Steam Venting due to Changing Core Exit Quality

As the rate of steam production increases, the quality of the two phase fluid leaving the core increases. This means the bubble content of the fluid is higher at higher reactor pressures. Because of the higher bubble content, the amount of steam contained in the fluid passing by the hot leg entrance is increased. This increase in steam entering the hot leg and leaving through the fourth stage ADS line can be a mechanism for

removing steam at a greater rate than steam production. This assumption can only be true if some of the steam in the upper head exits through the ADS4 line. This in fact is the case.

3.4.2 Changing Momentum in Exit Flow

If the exit flow were to increase over time due to a change in momentum, the positive rate of change of the bubble volume in the reactor would be conducive to a decrease in pressure. This requires that the volume of fluid in the exit pathways from the reactor be reasonably large. A large volume of fluid would require either a very long fourth stage ADS line or a very large flow area.

These conditions are not met in the APEX facility and a simple momentum analysis shows that the flow through the fourth stage ADS line can be represented rather well with a steady state Bernoulli equation.

If we look at the following equation,

$$F = ma, \quad (3.1)$$

and rewrite it using the differential form for acceleration,

$$F = m \frac{dv}{dt}, \quad (3.2)$$

we can solve for the velocity by using a rough approximation to the differential as shown in the following expression.

$$\frac{F\Delta t}{m} = v_t - v_{t-1} \quad (3.3)$$

This expression can be applied to the ADS4 line where;

m = the mass of liquid in the ADS4 line,

Δt = a given time step for the analysis,

v_t = the new velocity at the current time step,

v_{t-1} = the old velocity at the old time step,

F = the sum of the forces on the liquid in the ADS4 line which includes;

$P_1 A_1$ = Reactor pressure force applied at the entrance area to the ADS4 line,

$P_2 A_2$ = Sump pressure force applied at the separator entrance area,

kv_t^2 = Frictional force along the piping section using the fluid velocity,

ρgh = gravitational force required to lift the liquid from the hot leg elevation to the separator entrance elevation (h).

Applying all the definitions above, we arrive at the following expression.

$$\frac{[P_1 \pi r_{ADS4}^2 - P_2 \pi r_{ADS4}^2 - kv_t^2 - \rho gh \pi r_{ADS4}^2] \Delta t}{\rho L \pi r_{ADS4}^2} + v_{t-1} = v_t \quad (3.4)$$

Figure 3.7 shows the ADS4 liquid flow versus a simulated oscillating reactor pressure for actual APEX geometry and typical flow conditions. This plot shows the momentum of the fluid does not induce a time distortion in the flow when driven by the reactor pressure. This provides confidence in the use of a steady state formulation (Bernoulli's equation) to predict the ADS4 flow.

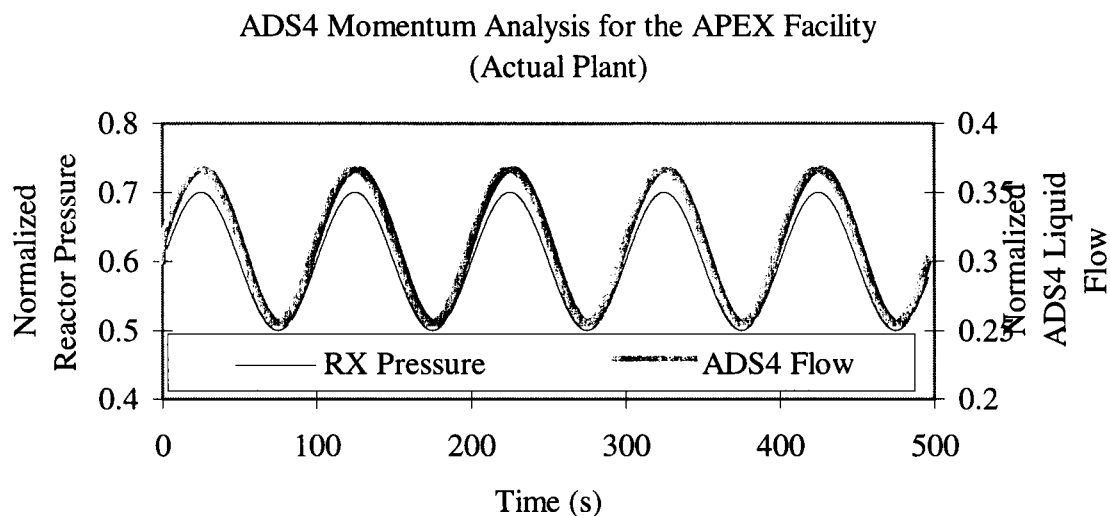


Figure 3.7 Figure showing the comparison between simulated pressure oscillations and ADS4 liquid flow oscillations. Notice how well the ADS4 flow follows the pressure.

When we change the mass in the line to five times the actual facility mass by fictitiously changing the length of the line, we can begin to see a lag in the flow versus the pressure as shown in figure 3.8.

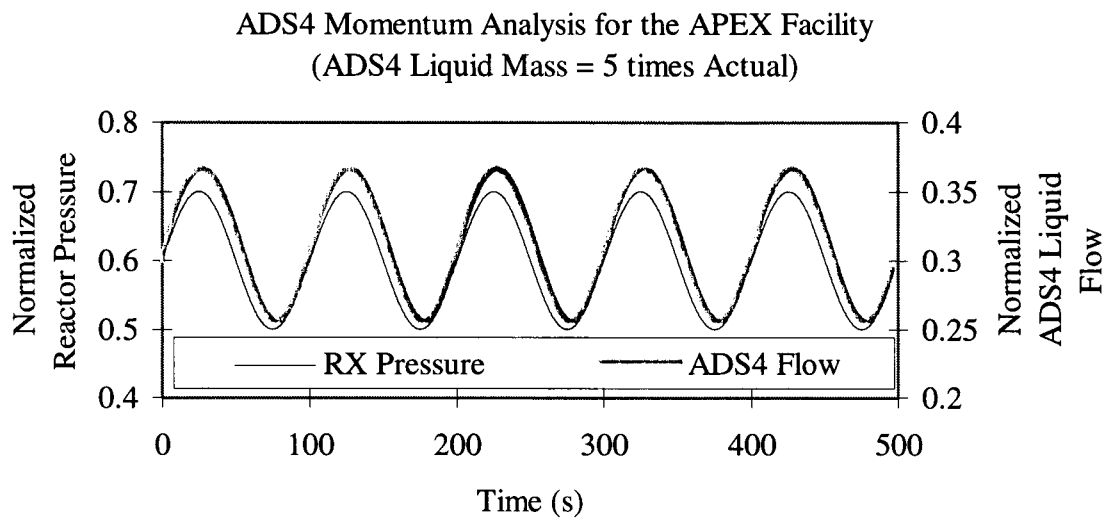


Figure 3.8 Figure showing the time lag between reactor simulated pressure and ADS4 flow for a fictitious ADS4 pipe length.

When we increase the mass to a very large value using an extremely long fictitious pipe length, we can see the momentum distortion clearly as shown in figure 3.9.

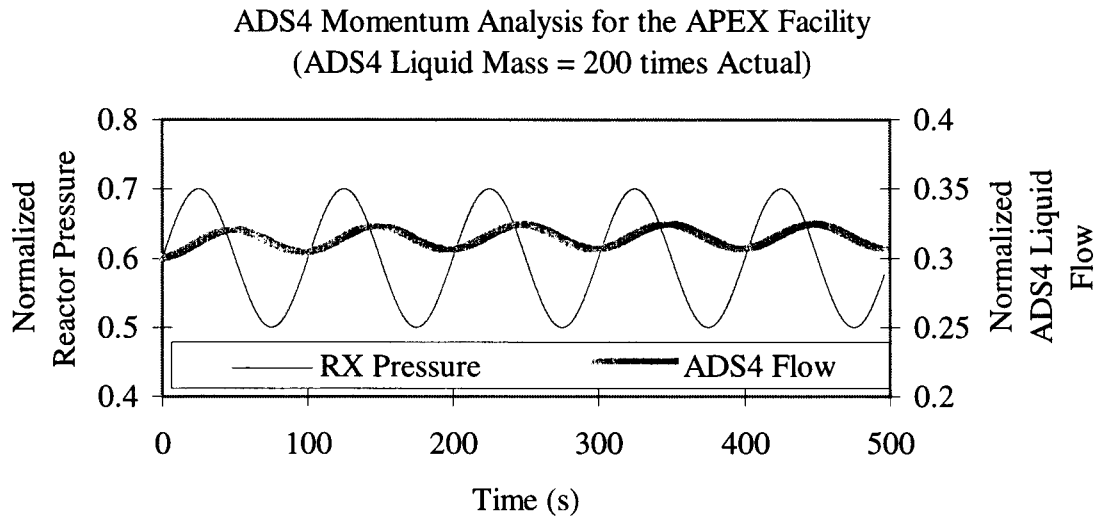


Figure 3.9 Momentum distortion for an extreme fictitious ADS4 pipe length and liquid mass.

3.4.3 Condensation in the Downcomer

Condensation does occur in the downcomer during the oscillations. Steam which has collected in the upper reactor head has a pathway through the downcomer bypass holes to flow down and condense on the cooler downcomer liquid. From the data, a simple energy balance shows a sizable fraction of the core power leaving with the break liquid. Conduction through the inside wall of the downcomer can't completely account for all of the energy leaving with the break fluid, therefore there is some condensation. Figures 3.10 and 3.11 show the energy flux contributions to the primary during a test (10).

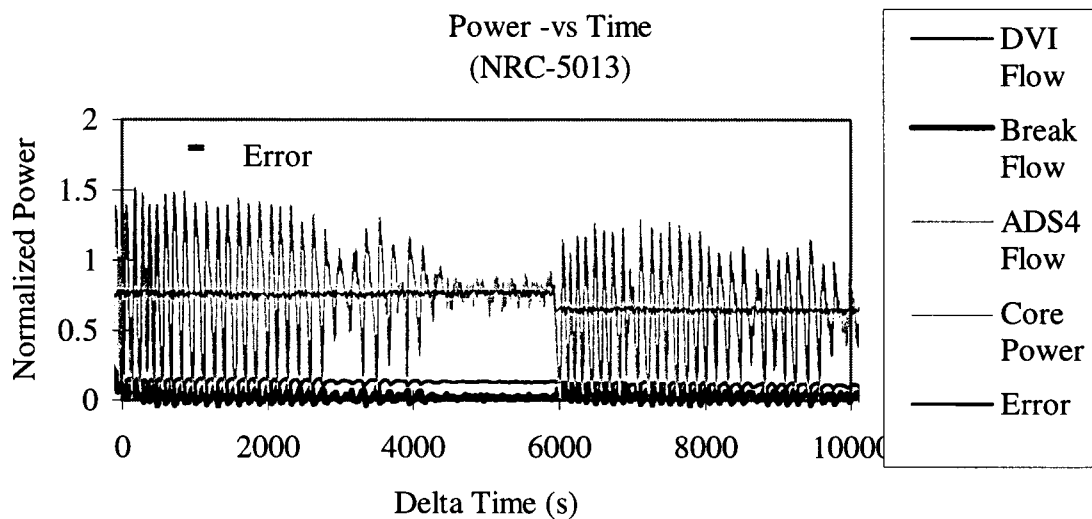


Figure 3.10 The energy percentage contributions for the RSO.

The sources of energy into the system were the core power and the energy of the DVI fluid. Energy leaving the system included the fluid energy through the break and the ADS4. Figure 3.11 shows the total energy in balanced the energy leaving the system.

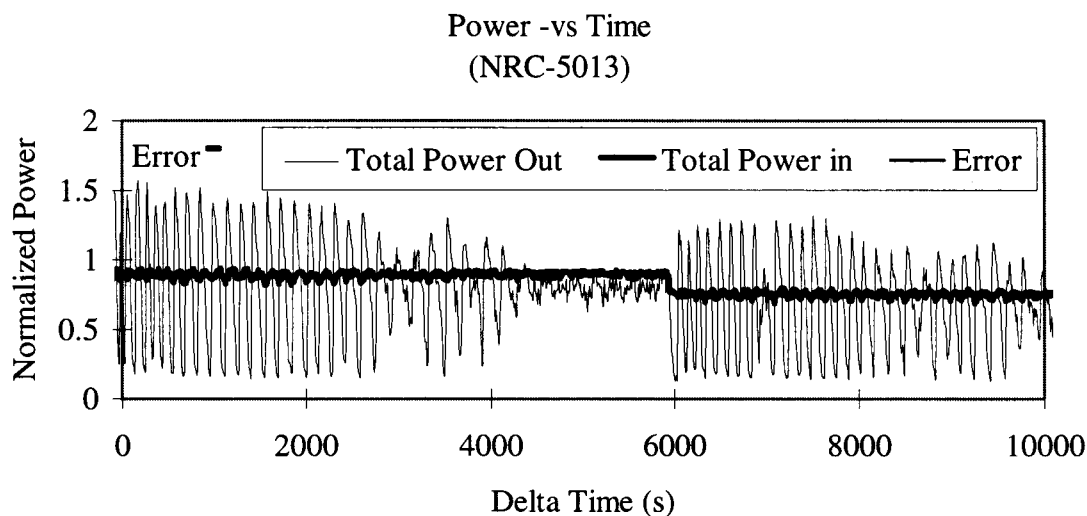


Figure 3.11 Total energy out of the primary system during the RSO.

3.4.4 Pressure Oscillation in the Sump

Pressure oscillations in the sump could be conducive to a changing exit flow. This changing exit flow could potentially cause a change in the size of the reactor steam bubble which would in turn change the pressure of the bubble. If this were the case, the sump pressure would have to be oscillating in sink with the oscillations in the core at the proper time. This has not been found to be the case as shown in figure 3.12.

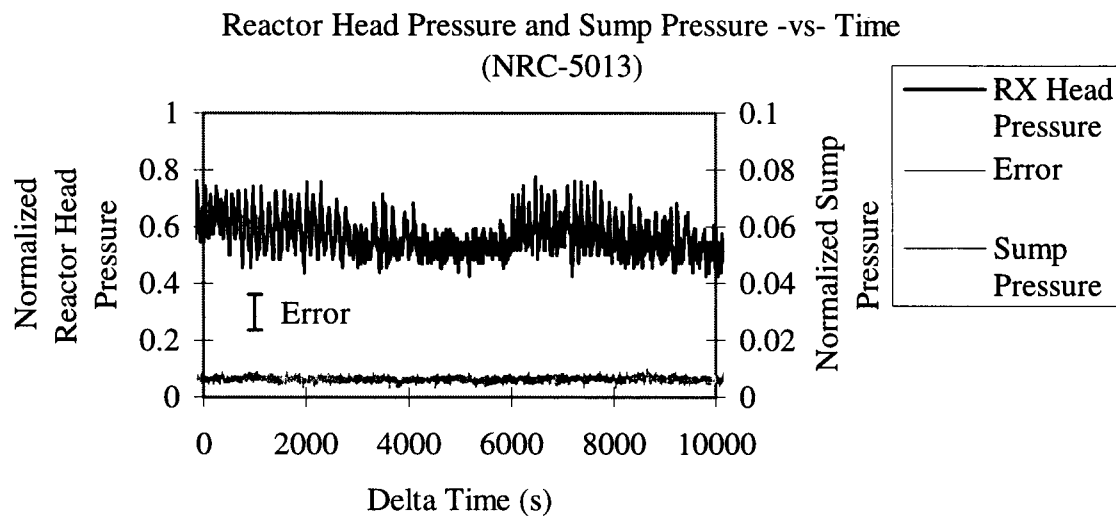


Figure 3.12 Pressure in the reactor head and primary sump during RSO.

4. Description of RSO Mechanisms

4.1 Introduction

The RSO is actually a sequence of events tied together. This chapter is dedicated to the explanation of each part of that sequence. One very interesting and critical note to mention is the apparent absence of steam leaving the reactor system during and after oscillations (10). Steam does leave the reactor in very small quantities (levels below our instruments capability to measure) and in small chaotic bursts but a simple energy balance shows primary system energy fluxes can be tracked through liquid inventories alone. Additional instrumentation was installed on the ADS4 and break lines leaving the system to enhance the facility's capability to measure steam venting through those systems (10). Further analysis indicates that steam must leave the reactor through the ADS4 line. This particular requirement is proven by photographic evidence. A careful study of the relative elevations of the IRWST liquid level and the ADS4 line elevations reveals that no flow is possible through the ADS4 (during oscillations) unless there is a two-phase flow. The two-phase flow decreases the density of the fluid in the ADS4 line allowing liquid to flow to the ADS4 separators. Indeed when looking at data, there is substantial liquid flow through the ADS4 lines during the oscillations when there is not enough driving head from the IRWST to make this possible without a two-phase condition in the ADS4 line.

The place to begin our explanation is before the oscillations start. RSO begins when the plant is well depressurized and injection water has entered the reactor system

at a rate fast enough to subcool the system. Figure 4.1 shows the APEX system before oscillation onset.

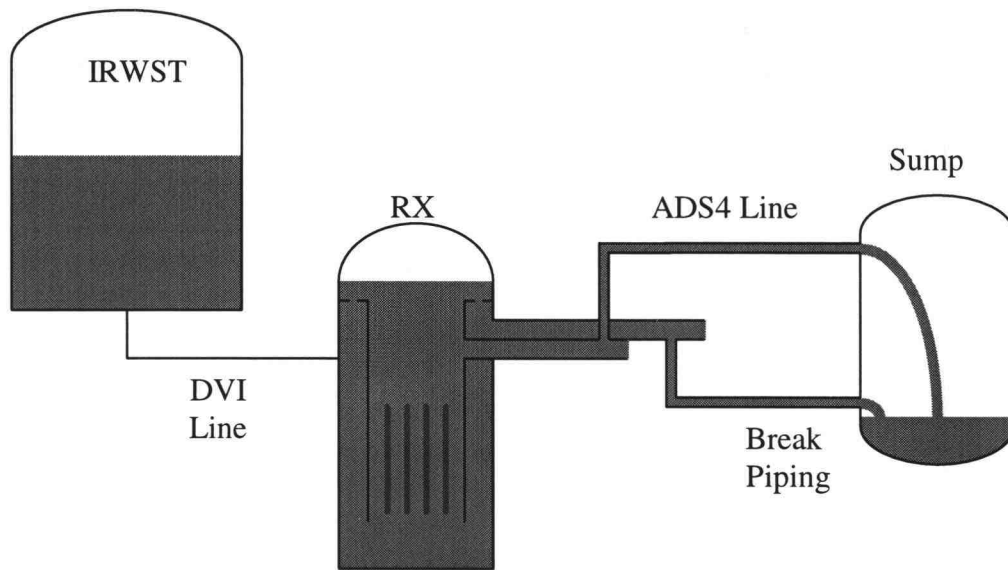


Figure 4.1 APEX system before oscillation onset.

Table 4.1 shows the six stages of the oscillations and the parameters that are important.

Stage	Boiling	TOHL	Pressure	DVI Flow	ADS 4 Flow	Break Flow
Pre	None	Covered	Minimum	Maximum	Stopped	Minimum
1	Minimum	Closes/Closed	Minimum	Maximum	Stopped	Minimum
2	Increasing	Covered	Increasing	Decreasing	Stopped	Increasing
3	Maximum	Opens	Maximum	Minimum	Maximum	Maximum
4	Decreasing	Open	Decreasing	Increasing	Decreasing	Decreasing
Post	Minimum	Remains Open	Minimum	Maximum	Steady	Minimum

Table 4.1 Stages of RSO.

4.2 Pre RSO

As the IRWST drains into the reactor, the driving head of the IRWST decreases enough to allow fluid to become saturated at the reactor core exit. Allowing the core to become saturated and to begin boiling sets the stage for the oscillations. Steam boiling off the top of the core fills the reactor head, the cold legs, the steam generator cold plenums and part of the upper plenum. As this steam is flowing into those areas of the system, a little of the steam is condensed on some of the cooler liquid surfaces heating them up to saturation.

The general requirements for the oscillations have now been set up. The mean free liquid surface in the reactor has achieved an elevation where a vent path for steam can leave the ADS 4 train causing steam venting to become unstable. The following figure shows the APEX plant during stages one and two of the RSO.

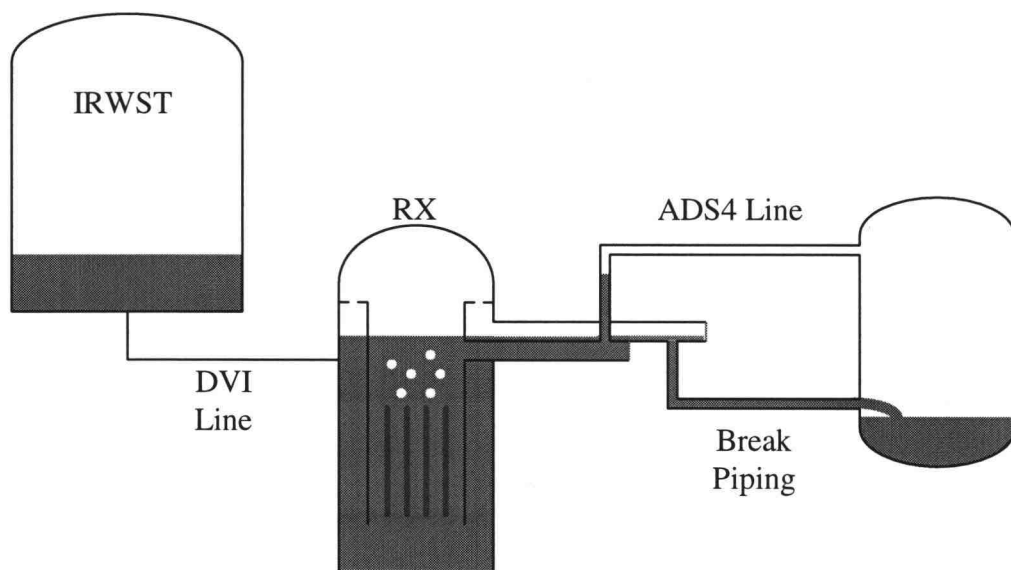


Figure 4.2 Stage 1 and 2. View of the APEX test facility when the oscillations begin. The ADS4 line is sealed with some standing water in the ADS4 line.

4.3 Stage One

The first stage of the oscillations is the lowest pressure point of the oscillation cycle. This is the point where the DVI flow is maximum, the ADS4 flow is stopped, and the break flow is minimum.

4.4 Stage Two

The second stage is a continuation of the first stage. As steam is generated at the core exit, the pressure in the reactor head is increasing. This increase in pressure is causing the DVI flow to decrease and the break flow to increase. The ADS4 flow is still zero because the top of the hot leg is still covered at this point.

4.5 Stage three

The third stage is the point where the reactor head pressure is equal to the gravity head of the liquid filled vertical section of the ADS 4 line. At this point, liquid begins flowing out of the hot leg and up the ADS4 line causing a flow instability at the entrance to the hot leg. This flow instability entrains some of the steam from the reactor head and a two-phase mixture develops in the ADS4 line.

4.6 Stage Four

The fourth stage of the RS oscillation is the continual depressurization of the primary system. The reactor head pressure now drops with the new steam vent pathway developed. As the pressure drops, the DVI flow rate begins to increase, the break flow

rate decreases and ADS 4 two-phase flow rate decreases. As the amount of liquid entering the primary system becomes larger than the amount of liquid exiting the system, the mean free liquid surface begins to increase in elevation.

Eventually the DVI flow will fill the reactor to the point of covering the top of the hot leg. With a decrease in primary pressure, the reactor can no longer drive liquid out of the ADS 4 line. When the system arrives at this condition, the ADS4 vent pathway is closed and the system then proceeds back to the first stage of the oscillation.

Figure 4.3 shows the APEX facility during stages three and four of the RSO.

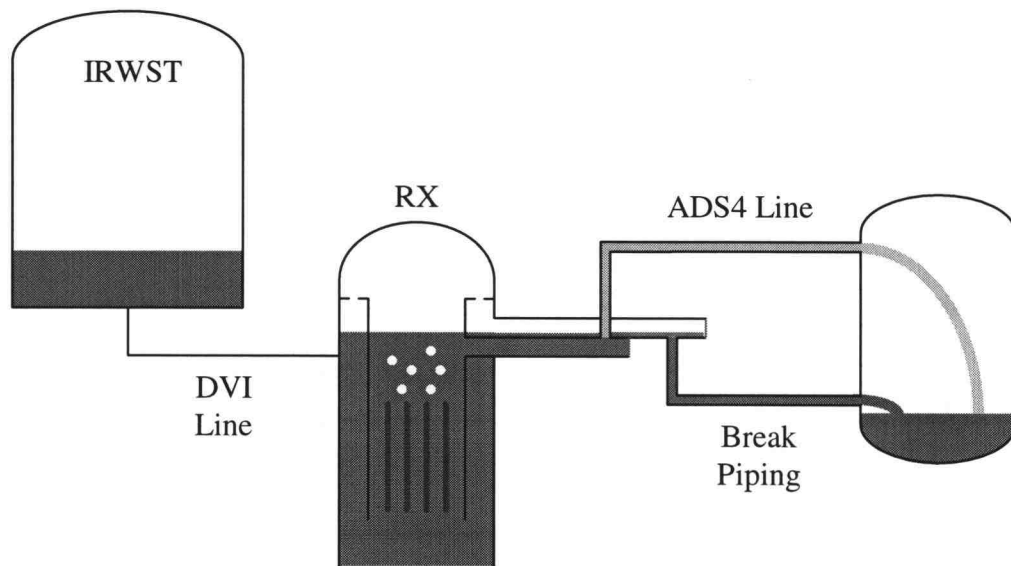


Figure 4.3 Stages 3 and 4. This figure shows the liquid inventory conditions for the plant at the point when ADS4 begins to flow with a two-phase mixture.

4.7 Termination

Termination of the oscillation occurs when two specific conditions are met. The DVI flow equals the liquid flow entrained in the ADS 4 line at the low pressure point of the oscillation and the total reactor liquid inventory is below the top of the hot leg elevation. A more detailed explanation for termination is explained in the next chapter.

Figure 4.4 shows the APEX plant at the point of RSO termination.

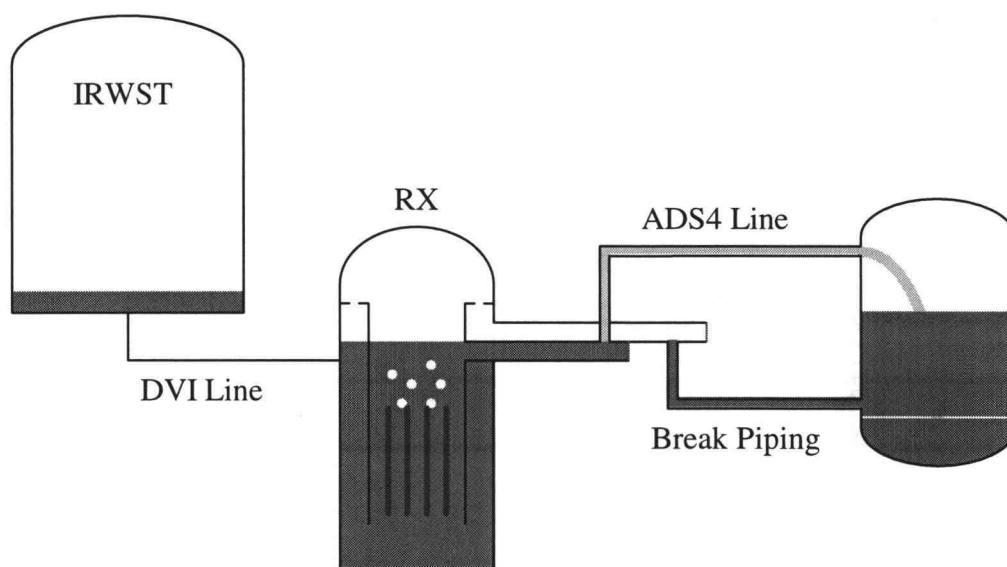


Figure 4.4 Oscillation termination.

Throughout the entire procession of the RSO, the reactor level never substantially drops below the top of the hot leg. This fact leads to the conclusion that RSO has no safety impact on the reactor inventory or core uncover. RSO cannot cause core uncover.

5. Oscillation Characteristics

5.1 Introduction

The RSO has many characteristics which need to be addressed. The following categories of onset, termination, period, amplitude, and barrel recirculation patterns are very important in understanding the oscillations. Understanding these particular characteristics can lead to a better understanding for scaling to the full sized plant.

5.2 Onset

Onset which has been explained previously can be explained in terms of a return to saturation conditions at the barrel exit. This particular characteristic would exist in the real AP600 plant and can be predicted easily using plant geometry, core power, and fluid properties.

5.3 Termination

Termination of the oscillation is one of the more difficult characteristics of the oscillations both in understanding and explanation. It is easiest to lay down rules which must be followed in order for the oscillations to terminate.

Rule 1.) The pressure in the reactor head must attain a state in which it no longer oscillates.

Rule 2.) In order for rule number one to exist, the steam density in the reactor steam volume must remain relatively constant.

We know from data that the steam volume in the reactor remains relatively unchanged (10,11,12). This same situation would occur in the full scale plant. Taking this assumption into account, we can make the next rule.

Rule 3.) The amount of steam produced must equal the amount of steam being vented at and after termination.

Rule number three is really the crux of the termination. Steam venting occurs in the oscillation at the higher pressures of the oscillation swing. Steam venting stops completely at the low pressure end of the oscillation because the amount of liquid above the top of the hot leg can seal off the vent path. If the vent path is sealed, then rule number two and three is violated and oscillations continue. Knowing that the liquid inventory is critical to rule number two in terms of keeping the steam density constant, we need to make another rule.

Rule 4.) The amount of liquid entering the reactor needs to be equal to the amount of liquid leaving the reactor when the reactor level approaches the top of the hot leg elevation.

This rule cinches up the slack in predicting the point of termination. The termination pressure is somewhere around the bottom of the pressure swing, near atmospheric pressure. To maintain rule number four, the amount of liquid entrained in the ADS4 lines must equal the amount of liquid injected through the DVI lines.

Using all the rules, and knowing how the plant behaves, we can make the following statement. Termination occurs when the steam generation rate is high enough at the minimum oscillation pressure for liquid entrainment in the ADS4 line to equal the DVI injection rate. Choosing a quality in the ADS4 line provides the conditions

necessary to plot the termination condition as shown in figures 5.1 and 5.2 (10). The core power is directly related to the amount of steam generation and the quality can predict the amount of liquid entrainment. Scaling this phenomenon to the real plant is very difficult. Different geometry leading to different head losses in the ADS4 lines can lead to difficulties in determining the ADS4 quality. The governing equations for figures 5.1 and 5.2 are developed in the next chapter.

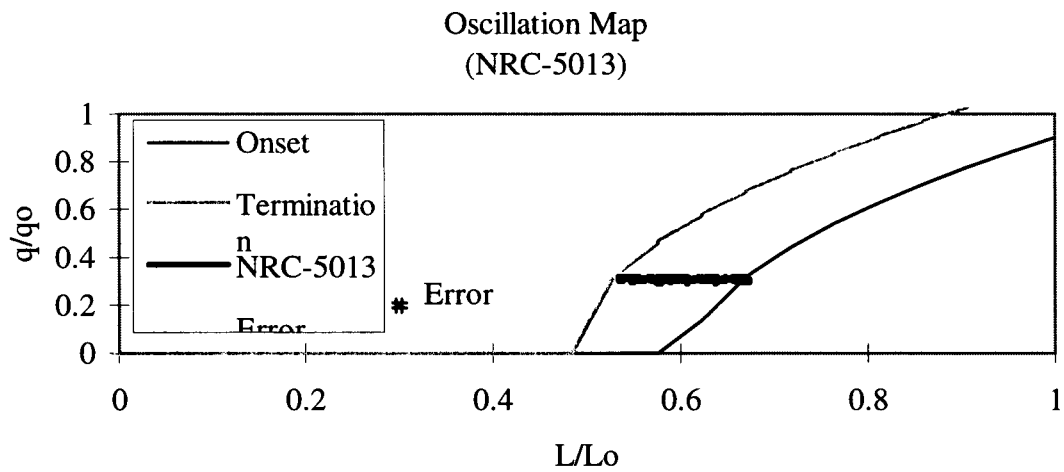


Figure 5.1 Plot showing onset and termination with APEX oscillation data for test NRC-5013.

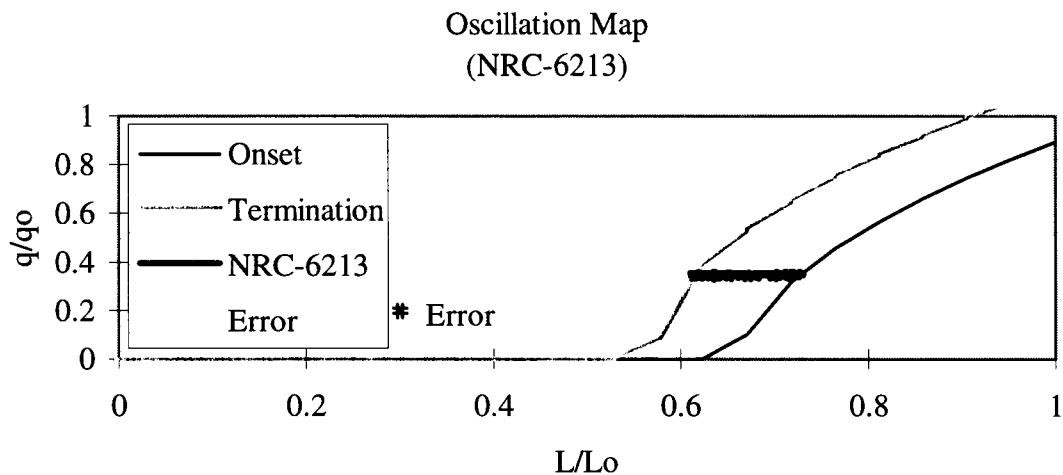


Figure 5.2 Plot showing onset and termination with APEX oscillation data for test NRC-6213.

5.4 Period

The period of the oscillations can be related to the rates at which steam can be vented and generated in the system. At the beginning of the oscillation, it is possible to see the break flow entraining a significant portion of the reactor energy. If this energy is leaving the reactor vessel, it is easy to believe that some of the steam generated in the core is being consumed by condensation along the barrel wall next to the downcomer and on the free liquid surface in the downcomer itself. This small amount of condensation is a removal mechanism to aid in the depressurization of the reactor and thus the periods are somewhat shorter than later in the oscillation. Later in the oscillation, the period stretches out due to the lack of break flow and the sump interaction.

When the break flow stops, the rate of steam condensation is reduced. If there is no longer a condensation mechanism, the steam which was condensed must now leave through the ADS4 lines and that takes more time; extending the period.

5.5 Amplitude

The amplitude of the oscillations are very straight forward. Pressure governs the oscillations. That is, pressure controls the ADS4 flow, the break flow, and the DVI flow. Therefore it is prudent to understand the pressure amplitude.

The lowest pressure in the oscillation is atmospheric pressure plus some small head loss through the steam exit pathways. The high end of the oscillations can be easily predicted by determining the ADS4 elevation head. There is some additional head loss which can be added to the oscillation high pressure but it is very small.

5.6 Recirculation patterns in the barrel

It is typically reasonable to assume that all of the energy released in the saturated region of the core can be used to generate steam. However when studying the data, we find that there is almost no steam leaving the reactor vessel. Almost all of the energy entering and leaving the system could be accounted for using liquid flow rates and core power rather than any steam measurements (i.e. all the energy leaving the system was leaving in the form of hot liquid instead of steam or a two phase mixture of steam and liquid where steam was not a contributing energy factor as shown in figures 5.3).

This poses a problem because the data shows the upper one third portion of the core is saturated (10,11,12). For the APEX testing facility, the power profile dictates

that half of the core power is expended in this region. If up to one half the core power is transferred into a saturated region, one can calculate a large volume of steam being produced in the reactor vessel which is not vented from the primary system according to data.

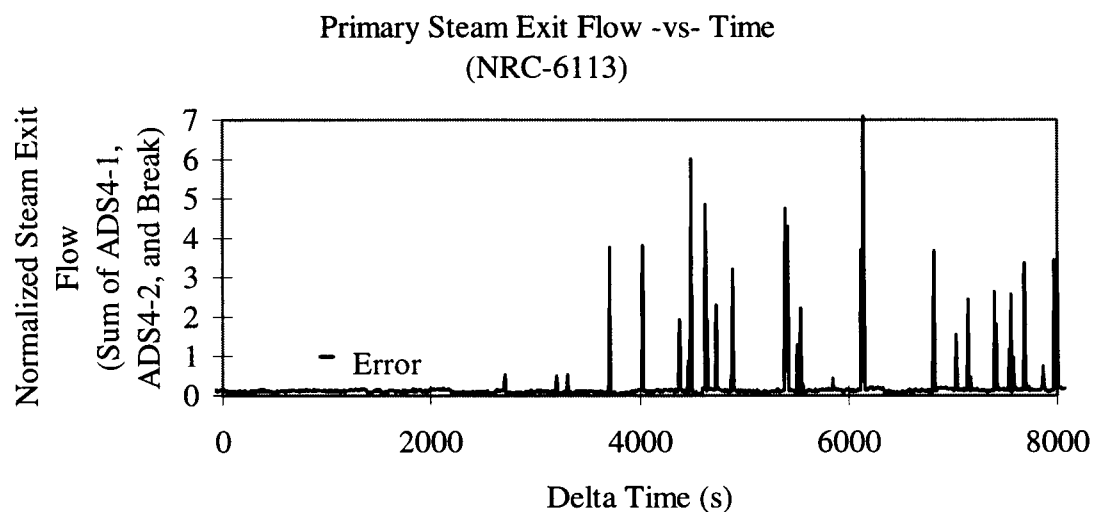


Figure 5.3 APEX data showing steam exiting the reactor through the break and ADS4 lines during RSO.

Careful study of the radial temperature profiles from data show a temperature dip in the center of the core as shown in Figure 5.4.

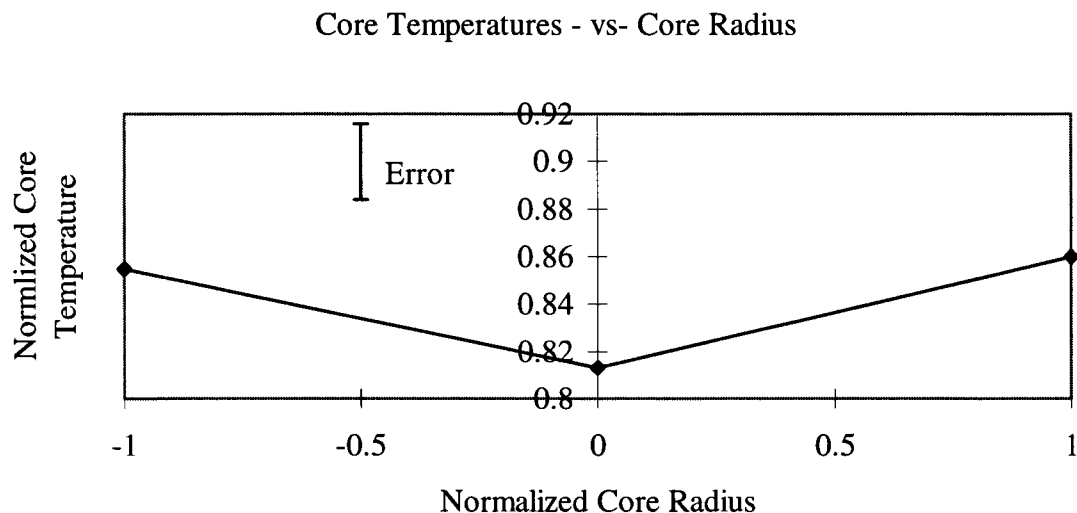


Figure 5.4 APEX data showing the temperature depression in the center of the reactor core.

When discussing the periods of the oscillations, condensation occurring on the inside wall of the barrel (heat was leaving the barrel and entering the colder liquid in the downcomer through the barrel wall) was mentioned. It is believed that this initial phenomenon initiates an interesting three dimensional flow pattern in the reactor causing an upwelling of colder liquid in the center of the reactor. The temperature data suggests that this phenomenon exists and this unforeseen circulation pattern in the reactor causes much of the steam to be condensed, or the rate of steam generation greatly reduced.

6. Numerical Analysis of the Oscillations (APOS Code)

6.1 Introduction

The easiest method to predict the oscillation period, frequency, onset, and termination is to use a numerical approach. One of the biggest advantages of this approach is the simplicity of building the conditions around the specific point of interest. For this discussion, the point of interest is the pressure in the reactor head.

To solve for a time dependent solution to the IRWST injection flow, the exit pressure of the system (along with the other parameters such as source surface elevation, source surface pressure, flow line data, etc.) would have to be known. The same requirements for determining the exit flow holds true for injection water.

Attempting to solve for the pressure in the reactor head would (at the very least) require the simultaneous solution for the head pressure, the injection flow, the exit flows, and potentially for several other parameters (core quality, flow split, etc.). Performing a numerical analysis allows for each of these things to be solved on a step by step basis.

6.2 General Descriptions of the APOS Code

Because of the previous discussion, a computer code has been written to simulate the oscillations. The code has been called the Apex Plant Oscillation Simulator or APOS. For simplicity the code has been written in the Excel (13) visual basic platform.

6.3 APOS Code General Assumptions

In writing the code, several assumptions were made in order to simplify the calculation. These assumptions are listed below.

6.3.1 Injection and Exit Flows

To calculate the injection and exit flows, a simple Bernoulli equation is used. This simplification makes a time dependent solution for these flows irrelevant due to the known head pressure at the current time step. The discussion presented in section 3.4.3 has shown that a time dependent momentum analysis for injection and exit flow is not necessary. Friction values for injection and exit flows were calculated using test data obtained in the APEX program (14).

6.3.2 Core Temperature Profile

The APEX temperature profile is different than that of a regular power plant (15). The profile is a skewed cosine profile with two-thirds of the power in the top half of the core. This modification was done in order to produce worst case scenarios during testing. The profile in the facility is hard wired and cannot be changed. Given the power profile, the core axial temperatures have been determined using a transient energy balance.

6.3.3 The Perfect Gas Assumption

In order to model the pressure in the steam bubble, the perfect gas law has been employed as the governing equation for pressure. Typically the perfect gas law fails when the working gas is close to a condensation point or near the state of a plasma. However using the perfect gas law carefully (being careful to note volumes and temperatures) the perfect gas law works with reasonable accuracy.

6.4 Governing Equations of the APOS Code

The following section will describe the equations and nodes used in the APOS code. Figure 6.1 is the nodalization diagram for APOS. Node 1 is a control volume for the IRWST. Node 2 models both DVI lines. Node 3 is a control volume that includes the lower downcomer and lower reactor plenum. Node 4 consists of 20 sub-nodes for calculations of the temperature distribution in the core. Node 6 includes the upper plenum; above the top of the core extending above the hot leg and can change its size accordingly to true liquid inventories. Node 5 is the upper head steam control volume and Node 7 is the ADS4 line.

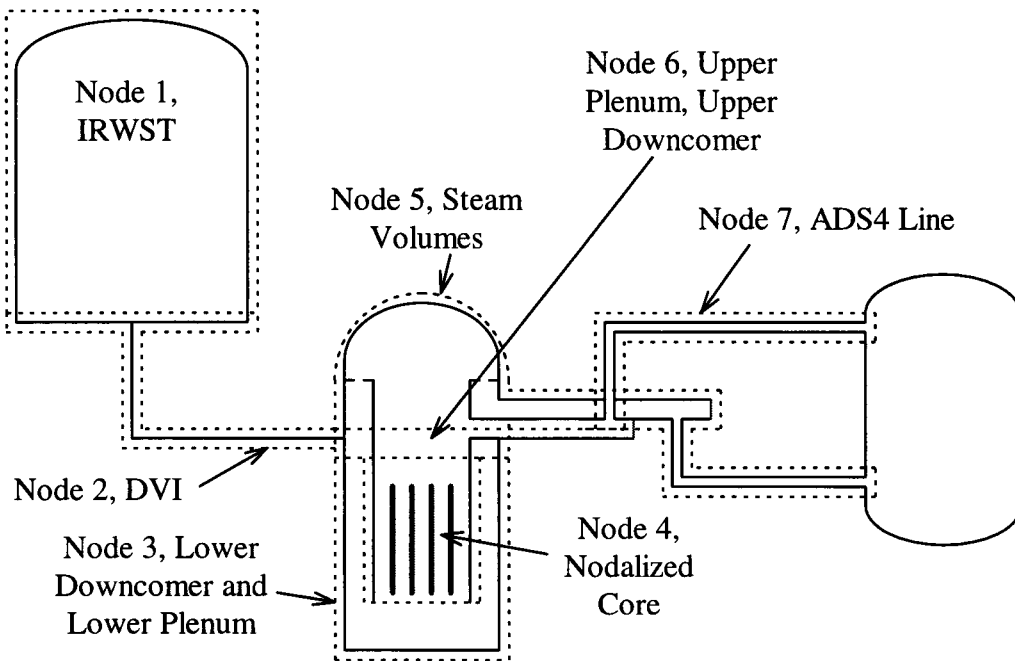


Figure 6.1 Components of the RSO

The governing equations for the APOS code are presented here in a fashion which describes the model at a general time step.

6.4.1 Node 1, IRWST Equations

The transport phenomenon of interest in the IRWST is governed by the liquid mass conservation equation. Performing a liquid mass balance for the IRWST control volume determines the level in the tank at a given time. Knowing the level in the tank provides us with the parameters needed to determine the pressure at the IRWST

injection line inlet. The analysis begins with the general form of the integral mass balance equations (16).

$$\frac{\partial}{\partial t} \iiint_{c.v.} \rho dV + \iint_{c.s.} \rho (\vec{v} \cdot \vec{n}) dA = 0 \quad (6.1)$$

Assumptions:

- 1.) During the IRWST injection phase, the amount of mass contributed by the ADS 1-3 trains is negligible.
- 2.) The fluid is incompressible therefore density is constant.
- 3) The only term causing any change in the IRWST inventory is the liquid flow rate out of the two IRWST injection lines. There is no mass flow into the IRWST at the point of RSO.
- 4.) The IRWST is cylindrical and of fixed radius.

Applying assumptions one through four to equation 6.1 yields the following.

$$\rho A_{IRWST} \frac{d z_{IRWST}}{d t} = -\dot{m}_{inject} \quad (6.2)$$

Integrating to solve for the liquid level for a given time step results in the following expression.

$$z_{IRWST, i} = z_{IRWST, i-1} + \frac{(\dot{m}_{inject, i-1} \Delta t)}{\rho_f A_{IRWST}} \quad (6.3)$$

6.4.2 Node 2, DVI Line Equations

The transport phenomenon of interest in the DVI lines is governed by the liquid energy conservation equation. Performing an energy balance on the DVI control volume determines the mass flow rate through the DVI line. The analysis starts with the general form of the integral energy equation.

$$\frac{\delta Q}{dt} - \frac{\delta W_s}{dt} = \iint_{c.s.} \left(e + \frac{P}{\rho} \right) \rho (\vec{v} \cdot \vec{n}) dA + \frac{\partial}{\partial t} \iiint_{c.v.} e \rho dV + \frac{\delta W_\mu}{dt} \quad (6.4)$$

Assumptions:

5.) The DVI lines remain full during IRWST draining, material properties are constant, and the momentum of the mass of liquid in the DVI lines is small enough to make any momentum effects negligible.

$$\frac{\partial}{\partial t} \iiint_{c.v.} e \rho dV \cong 0 \quad (6.5)$$

6.) There is no heat transfer in the DVI line.

$$\frac{\delta Q}{dt} = 0 \quad (6.6)$$

7.) The fluid in the DVI lines is incompressible.

8.) There is no viscous work at the control surfaces.

$$\frac{\delta W_\mu}{dt} = 0 \quad (6.7)$$

9.) There is no shaft work performed in the DVI control volume.

$$\frac{\delta W_s}{dt} = 0 \quad (6.8)$$

10.) The fluid and flow properties (material properties and fluid velocities) are constant across the control surfaces in the DVI line.

The analysis now uses the following definitions:

Specific Total Energy:

$$e = u + \frac{v^2}{2} + gz \quad (6.9)$$

where u = internal energy, $v^2/2$ = kinetic energy, and gz is the potential energy.

Change in Internal Energy:

$$\Delta u = h_L g \quad (6.10)$$

where h_L is the friction and form head loss.

The mass conservation equation for an incompressible fluid flowing at steady-state conditions is written in the following form.

$$v_1 A_1 = v_2 A_2 \quad (6.11)$$

Applying assumptions five through nine to the energy equation yields the following.

$$\iint_{c. s.} \left(e + \frac{P}{\rho} \right) (\vec{v} \cdot \vec{n}) dA = 0 \quad (6.12)$$

Applying assumption ten and integrating for an inlet control surface 1 at the IRWST injection line entrance and an outlet control surface 2 at the DVI exit yields the following expression.

$$\left(e + \frac{P}{\rho} \right)_2 v_2 A_2 - \left(e + \frac{P}{\rho} \right)_1 v_1 A_1 = 0 \quad (6.13)$$

Substituting equation 6.9 into equation 6.13 and using equation 6.11 yields the next equation.

$$\left(u + \frac{v^2}{2} + gz + \frac{P}{\rho} \right)_1 = \left(u + \frac{v^2}{2} + gz + \frac{P}{\rho} \right)_2 \quad (6.14)$$

Moving the internal energy terms to the right side and applying equation 6.10, dividing through by g , the following expression can be derived.

$$\frac{P_1}{\rho g} + \frac{v_1^2}{2g} + z_1 = \frac{P_2}{\rho g} + \frac{v_2^2}{2g} + z_2 + h_L \quad (6.15)$$

The analysis defines the head loss in terms of the kinetic energy of the fluid by using the following expression (16).

$$h_L = k \frac{v_2^2}{2g} \quad (6.16)$$

The parameter k is a dimensionless friction and form loss group based on the geometry and internal surface roughness of the piping. The value of k is measured experimentally and given by the following expression.

$$k = \sum_{i=1}^N \left[\left(\frac{f\ell}{D} + K \right)_i \left(\frac{A_2}{A_i} \right)^2 \right] \quad (6.17)$$

In equation 6.17, f is the Darcy surface friction factor (16), d is the inside diameter of the piping, ℓ is the pipe length, K is the form loss coefficient, A_2 is the cross-sectional flow area of a single DVI line and A_i is the cross-sectional flow area of the individual sections that comprise the IRWST and DVI injection lines. Measurements indicate that the loss coefficients, K_i , dominate the pressure drop in the piping. Implementing equation 6.16 in equation 6.15 yields the modified Bernoulli equation.

$$\frac{P_1}{\rho g} + \frac{v_1^2}{2g} + z_1 = \frac{P_2}{\rho g} + \frac{v_2^2}{2g} + z_2 + k \frac{v_2^2}{2g} \quad (6.18)$$

To solve for the velocity in the DVI line, equations are needed for v_1 , P_1 , and P_2 . The following assumptions will be used to obtain those relationships.

11.) The inlet velocity, v_1 is small compared to the velocity in the DVI, therefore v_1 is set to zero.

$$v_1 = 0 \quad (6.19)$$

12.) The analysis assumes no pressure change due to head loss from the flow pathway connecting the top of the reactor head to the DVI entrance. P_2 can now be expressed in terms of the hydrostatic head equation.

$$\frac{dP}{dz} = -\rho g \quad (6.20)$$

The pressure at the DVI exit is equal to the pressure in the reactor head plus the gravity head of liquid above the exit. Integrating equation 6.20 and applying the proper elevations, the following expression for P_2 is derived.

$$\frac{P_2}{\rho g} = \frac{P_{RX,i}}{\rho g} + z_{RX,i} - z_2 \quad (6.21)$$

In a similar manner, integrating equation 6.20 expresses the pressure at the IRWST injection line inlet.

$$\frac{P_1}{\rho g} = \frac{P_{IRWST,i}}{\rho g} + z_{IRWST,i} - z_1 \quad (6.22)$$

13.) Because the IRWST free surface is at room pressure, it is possible to set P_{IRWST} to zero gauge eliminating it from equation 6.22.

Substituting equation 6.19, 6.21 and 6.22 into equation 6.18 and applying assumption 13, the following velocity term in one DVI line is produced.

$$v_{DVI, i} = \sqrt{\frac{\left[z_{IRWST, i} - z_{RX, i} - \frac{P_{RX, i}}{\rho g} \right] 2g}{1 + k_{DVI}}} \quad (6.23)$$

The code uses a logic statement which says if the term under the radical is positive, a flow exists in the DVI lines. If the radical term is negative the code sets the DVI velocity to zero. This is a true representation in the plant considering the check valves in place for the design.

Multiplying the DVI velocity by two (for two DVI lines), the density of the IRWST injection water and the cross sectional area of the DVI line, we can determine the injection mass flow rate can be determined.

$$\dot{m}_{inject, i} = 2\rho v_{DVI, i} \frac{\pi D_{DVI}^2}{4} \quad (6.24)$$

6.4.3 Node 3, Downcomer Below DVI and Reactor Lower Vessel Plenum

The phenomenon of interest in the Lower downcomer and lower vessel plenum is the mass conservation. Although the code does not directly keep track of the liquid inventory, the logic used connecting of the DVI to the bottom of the core requires mention.

Assumptions:

- 14.) The liquid in the lower downcomer and lower vessel plenum is incompressible.
- 15.) The only pathways for fluid to enter and exit this node are the DVI lines, the break and the bottom entrance to the reactor core.

- 16.) The density change with respect to temperature is small and is therefore neglected.
- 17.) The control volume is always full during RSO, therefore there is no mass accumulation.

Applying assumptions 14 through 17 to equation 6.1, we can solve for the mass flow rate relationship.

$$\dot{m}_{\text{core}} - \dot{m}_{\text{break}} - \dot{m}_{\text{inject}} = 0 \quad (6.25)$$

6.4.4 Node 4, The Nodalized Core (20 core nodes)

The phenomenon of interest concerning the core is the amount of steam produced. An important step in the calculation is to determine how much heat from the bundle is being used to produce steam. In order to make a reasonable determination of this parameter, it is necessary to determine the axial location in the core where the water becomes saturated. The saturation line in the core is strongly affected by the power profile, core flow rate, and entrance temperatures.

Due to the transient nature of the core flow rate (caused by pressure oscillations changing the injection flow rates), a steady state type of analysis cannot capture the true behavior of the core temperature profiles. In order to model the core temperature profiles, the core was nodalized into twenty equal sized nodes.

In this algorithm, each node is identical except for the bottom node. The only difference for the bottom node is the temperature of the liquid entering that node from

the lower plenum is fixed to the injection temperature and not the temperature of a node beneath it.

6.4.4.1 Core Nodes at Subcooled Conditions

The goal is to determine the saturation elevation in the core. The first step is to solve for the temperature profile in the subcooled region of the core. It is easiest to begin with equation 6.4, the integral energy equation.

Assumptions:

- 18.) Density is constant for all regions and all temperatures.
- 19.) No shaft work.
- 20.) No viscous work at the control surface.
- 21.) Uniform fluid properties at the control surface.
- 22.) It is assumed that the cross sectional fluid temperatures in the core are homogenized.

The analysis applies the following definitions.

Specific Internal Energy Change:

$$du = C_v dT \quad (6.26)$$

Specific Enthalpy Change:

$$dh = C_p dT \quad (6.27)$$

Specific Enthalpy

$$h = u + \frac{P}{\rho} \quad (6.28)$$

Nodal Power:

$$q_{\text{node}} = \frac{\delta Q}{dt} \quad (6.29)$$

Applying assumptions 18 through 22 to equation 6.4 and integrating over the control surfaces for one node, the following can be derived.

$$\frac{\delta Q}{dt} = \left(e + \frac{P}{\rho} \right)_{\text{out}} \dot{m}_{\text{out}} - \left(e + \frac{P}{\rho} \right)_{\text{in}} \dot{m}_{\text{in}} + M_{\text{node}} \frac{de}{dt} \quad (6.30)$$

The analysis makes the following assumptions:

23.) The total energy (e) is composed of kinetic, internal, and potential energies. Changes in kinetic and potential energy are negligible compared to changes in internal energy, therefore the total energy (e) in equation 6.30 can be represented by the internal energy (u).

24.) For the subcooled region of the core, there is no mass accumulation. Therefore the mass conservation equation for each node can be expressed as follows.

$$\dot{m}_{j,i} - \dot{m}_{j-1,i} = 0 \quad (6.31)$$

therefore

$$\dot{m}_{j,i} = \dot{m}_{j-1,i} = \dot{m}_{\text{core},i} \quad (6.32)$$

Applying the definition for nodal power, specific enthalpy, assumption 23 and assumption 24, the following can be derived.

$$M_{\text{node}} \frac{du_j}{dt} = \dot{m}_{\text{core},i} \left[(h)_{j-1,i-1} - (h)_{j,i-1} \right] + q_{j,i} \quad (6.33)$$

Integrating equation 6.27 and substituting this result and equation 6.26 into equation 6.33 yields the following.

$$M_{\text{node}} C_v \frac{dT_j}{dt} = \dot{m}_{\text{core}} C_p (T_{j-1,i-1} - T_{j,i-1}) + q_{j,i} \quad (6.34)$$

Integrating equation 6.34 and solving for T_j , yields the following expression for the mixture temperature in the node.

$$T_{j,i} = \frac{\Delta t \left[\dot{m}_{\text{core}} C_p (T_{j-1,i-1} - T_{j,i-1}) + q_{j,i} \right]}{M_{\text{node}} C_v} + T_{j,i-1} \quad (6.35)$$

The temperature change due to the amount of power dumped into the node is now calculated. Using the power rate generated at the center of the node and multiplying that by the node length, it is possible to determine the node power (15).

$$q_{j,i} = 3.11 q'_{\text{avg}} \Delta z \left(\frac{z_j}{L} \right) \left(1 - \frac{z_j}{L} \right)^{\frac{1}{3}} \quad (6.36)$$

6.4.4.2 Core Nodes at Saturated Conditions

When the temperature profile of all the nodes is calculated, the number of nodes that have reached saturation temperature are counted. Multiplying the number of nodes that have reached saturation by the node length provides us the length of the boiling region in the core. Integrating equation 6.36 over the saturated length yields the equation used to determine the amount of core power used to generate steam.

$$q_{\text{steam}, i} = 9.33 q'_{\text{avg}, i} L \left[\frac{\left(1 - \frac{z_{\text{sat}}}{L}\right)^{\frac{4}{3}}}{4} - \frac{\left(1 - \frac{z_{\text{sat}}}{L}\right)^{\frac{7}{3}}}{7} \right] \quad (6.37)$$

It is preferable to begin again with equation 6.4 for the entire saturated region of the core.

Assumptions:

- 25.) No shaft work.
- 26.) No viscous work at the control surfaces.
- 27.) The accumulation of internal energy and mass for the mixture is very small. The time dependence over a time step is small compared to the period of one oscillation.

The analysis employs the following definitions:

Inlet Enthalpy:

$$h_{\text{in}} = h_f \quad (6.38)$$

Outlet Enthalpy:

$$h_{\text{out}, i} = h_f + x_i h_{fg} \quad (6.39)$$

Vapor Quality:

$$x_{\text{core}, i} = \frac{\dot{m}_{\text{steam}, i}}{\dot{m}_{\text{core}, i}} \quad (6.40)$$

Power in the Saturated Region:

$$q_{\text{steam}, i} = \frac{\delta Q}{dt} \quad (6.41)$$

Applying assumptions 23, 25 through 27 and equations 6.28, 6.32, and 6.41 to equation 6.4 provides the following expression.

$$q_{\text{steam}, i} = \dot{m}_{\text{core}, i} \left[(h)_{\text{out}, i} - (h)_{\text{in}} \right] \quad (6.42)$$

Applying equations 6.38 through 6.40 to equation 6.42 and solving for the vapor generation rate yields the following.

$$\dot{m}_{\text{steam}, i} = \frac{q_{\text{steam}, i}}{h_{fg}} \quad (6.43)$$

6.4.5 Node 5, Steam Volumes

The phenomenon of interest in the steam volumes is the pressure. The steam volumes of the APEX test facility at the stage where RSO occurs encompasses the upper vessel plenum, reactor head, cold legs, cold steam generator plenums, and the majority of the u-tubes. All of these volumes are drained of liquid when the RSO begins.

Assumptions:

- 28.) No Heat transfer into or out of the steam volumes occurs. This means there is no condensation or boiling in the steam volumes.
- 29.) The temperature changes in the steam volumes will be negligible.
- 30.) Condensation and vaporization effects resulting from the small changes in saturation pressure are negligible.
- 31.) Changes in the size of the steam volumes are negligible over a single oscillation period, therefore the steam volumes will be considered to be a fixed size.
- 32.) The concentration of noncondensable gases present in the steam volumes is small enough to be neglected in the calculation.

The first step for an iteration is to determine the new pressure. The pressure at time step i is equal to the pressure at time step $i-1$ plus the change in pressure due to the amount of steam generated and vented from the system.

$$P_i = P_{i-1} + \Delta P_i \quad (6.44)$$

Using the ideal gas law, it is possible to determine the value of ΔP_i . Starting with the ideal gas law, rearranging and taking the derivative with respect to time, it is possible to arrive at an equation governing changes in steam pressure which are

dependent on time step, steam flow rates into and out of the control volume, the size of the control volume, steam temperature and the gas constant (17).

$$PV = MRT \text{ or } P = \frac{MRT}{V} \quad (6.45)$$

Taking the derivative with respect to time yields the following.

$$\frac{dP}{dt} = \frac{RT}{V} \frac{dM}{dt} \quad (6.46)$$

Applying equation 6.1 to the steam volume yields the following.

$$\frac{dM}{dt} = \dot{m}_{\text{steam}, i} - \dot{m}_{\text{steam vented}, i} \quad (6.47)$$

Substituting equation 6.47 into equation 6.46 and integrating provides the following.

$$\Delta P_{RX, i} = \Delta t \left(\dot{m}_{\text{steam}, i} - \dot{m}_{\text{steam vented}, i} \right) \frac{RT}{V} \quad (6.48)$$

This is the governing equation for pressure changes in the steam volumes. The mass flow rate of steam vented is expressed in the following equation.

$$\dot{m}_{\text{steam vented}, i} = x_{\text{ADS4}} \dot{m}_{\text{ADS4}, i} + \dot{m}_{\text{break}} \quad (6.49)$$

The modified Bernoulli equation given by equation 6.18 can be used to determine the break mass flow rate. Steam mass flow rates are calculated using the modified

Bernoulli equation to calculate liquid break flow and multiplying that number by an empirical constant derived from data to determine the steam condensation leaving the break. To determine the break flow, the following assumptions and definitions are utilized.

Reactor Head Pressure:

$$P_1 = P_{RX, i} \quad (6.50)$$

Sump Pressure:

$$P_2 = P_{sump, i} \quad (6.51)$$

Break Velocity:

$$V_2 = v_{break, i} \quad (6.52)$$

33.) Pressure is negligible for the geometry of the plant and liquid level conditions which are typically found at the time of the RSO. This allows the elevations in equation 6.18 to zero.

$$z_1 = z_2 = 0 \quad (6.53)$$

34.) The velocity v_1 is assumed to be zero.

Applying assumption 34 and substituting equations 6.50 through 6.53, equation 6.18 can be rewritten for the velocity of liquid through the break.

$$v_{\text{break}, i} = \sqrt{\frac{2g(P_{\text{RX}, i} - P_{\text{sump}, i})}{\rho_{\text{liquid}}(1 + k_{\text{break}})}} \quad (6.54)$$

Multiplying the break velocity by the liquid density of the injection flow, the cross sectional area of the break hole and the loss coefficient, k , determines the break mass flow rate.

$$\dot{m}_{\text{break}, i} = K_1 \rho v_{\text{break}, i} \frac{\pi D_{\text{break}}^2}{4} \quad (6.55)$$

K_1 is obtained from measurements at single-phase steady state conditions. Knowing the IRWST injection temperature and the break flow temperature, it is simple to determine the amount of steam condensed for that temperature change. Using a linear relationship with an intercept of zero, the slope of the line relating the condensation versus the break flow rate can be established. This is how K_1 is determined.

6.4.6 Node 6, Upper Plenum, Upper Downcomer.

The phenomenon of interest in the upper plenum and upper downcomer region is the mean free liquid surface elevation.

Assumptions:

35.) The liquid surface in the downcomer is at the same elevation as the collapsed liquid level in the upper plenum. This assumption is valid due to the bypass holes connecting the reactor upper head to the downcomer.

36.) The mean free liquid surface in the upper plenum is very close to the top of the hot leg (TOHL) when the ADS 4 begins venting steam. In reality, when the ADS 4 begins venting steam, the level is probably slightly higher than the TOHL. The analysis assumes the flow of liquid through the hot leg and out of the ADS 4 line creates a pathway that allows steam to leave the reactor.

In order to track the mean free liquid surface in node six, a simple liquid mass balance is performed over nodes three, four and six. The code treats the liquid inventories for nodes three and four as constant. The code also uses a parameter called the relative diameter.

The relative diameter is determined by calculating the total reactor cross sectional flow areas at the TOHL elevation (upper plenum area, downcomer area, and subtracting vessel internal structure cross sectional areas) and solving for the diameter of a circle of the same area.

Applying the following assumptions to equation 6.1 provides the expression describing changes in the upper plenum mean free surface elevation.

37.) The fluid is incompressible therefore density is constant.

38.) The only terms causing changes in the node six mass inventory is the liquid flow rate leaving through the ADS 4 line and the liquid flow rate entering through the DVI line.

39.) Node six is treated as cylindrical and of fixed radius.

The analysis also makes the following definition for the amount of liquid flowing out the ADS 4 line.

ADS 4 Liquid Mass Flow:

$$\dot{m}_{\text{out}} = (1 - x_{\text{ADS4}})\dot{m}_{\text{vent}, i} \quad (6.56)$$

Substituting the previous definition and applying assumptions 37 through 39 to equation 6.1 yields the following.

$$\rho_{\text{liq}} \frac{\pi D_{\text{rel}}^2}{4} \frac{d z_{\text{RX}, i}}{d t} = (\dot{m}_{\text{inject}, i} - (1 - x_{\text{ADS4}})\dot{m}_{\text{vent}, i}) \quad (6.57)$$

Integrating to solve for the liquid level for a given time step results in the following expression.

$$z_{\text{rx}, i} = z_{\text{rx}, i-1} + \left[\frac{(\dot{m}_{\text{inject}, i} - (1 - x_{\text{ADS4}})\dot{m}_{\text{vent}, i})}{\rho_{\text{liq}} \frac{\pi D_{\text{rel}}^2}{4}} \right] \Delta t \quad (6.58)$$

6.4.7 Node 7, ADS 4 Line

The phenomenon of interest in the ADS 4 line is the two phase fluid flow rate out of the primary system. The modified Bernoulli equation, 6.18, can be used to express the flow rate through the ADS 4 line.

Assumptions:

40.) The quality out of the ADS 4 line will be set by using equation 6.64.

To determine the amount of steam flowing through the ADS4 line, a certain amount of logic is required. The amount of steam flowing through the ADS4 line

changes over time. The fluid passing through the ADS 4 line changes quality (from a quality of zero to an average quality) with the RSO.

The condition of the liquid at the top of the hot leg is a critical point in determining ADS4 quality. The APOS model assumes the quality in the line is zero when the head pressure in the reactor is less than the gravity head plus an experimentally measured flow resistance in the ADS4 line. As the reactor head pressure reaches the elevation head plus flow resistance in the ADS4, the interface between the top of the hot leg and the ADS4 entrance begins to change. As the flow of liquid from the reactor starts flowing down the hot leg, the code assumes a pathway for steam is formed.

The flow of liquid out of the reactor exceeds the flow of liquid into the reactor, the mass flow rate of steam leaving the reactor exceeds the mass of steam being produced and the average liquid surface interface in the core begins to drop. The APOS code sets the ADS4 venting flag to “on” when the reactor head pressure exceeds the ADS4 gravity head plus flow resistance.

The amount of fluid venting through the ADS4 line is calculated using the same methodology used to develop equation 6.55. The ADS4 mass flow is multiplied by 1.5 to model one and a half ADS4 trains as built in the APEX facility.

$$v_{\text{ADS4}, i} = \sqrt{\frac{2g(P_{\text{RX}, i} - P_{\text{sump}, i})}{\rho_{\text{tp}}(1 + k_{\text{ADS4}})}} \quad (6.59)$$

$$\dot{m}_{\text{ADS4}, i} = 1.5 v_{\text{ADS4}, i} \frac{\pi D_{\text{ADS4}}^2}{4} \frac{\rho_{\text{tp}}}{g_c} \quad (6.60)$$

As the venting continues, more steam and liquid leave the reactor allowing the reactor head pressure to decrease. This decrease in head pressure increases the DVI flow and the liquid inventory eventually gets larger than the ADS4 liquid mass flow. As the mean liquid surface in the reactor begins to rise coupled with a lower reactor head pressure, the interface between the top of the hot leg and the ADS4 entrance becomes covered with slow moving liquid.

When the interface is re-covered (or the reactor liquid inventory exceeds the top of the hot leg elevation), the APOS code sets the ADS4 vent flag to “off” and one oscillation has been simulated.

One very important part of equation 6.60 is the calculation of ρ_{tp} . Starting with a general definition for density and vapor quality,

Density:

$$\rho = \frac{\text{mass}}{\text{unit volume}} \quad (6.61)$$

Vapor Quality:

$$x = \left. \frac{M_g}{M_g + M_f} \right|_{\text{given volume}} \quad (6.62)$$

an expression of two phase density can be solved.

$$\rho_{tp} = \frac{1}{\frac{x}{\rho_g} + \frac{1-x}{\rho_f}} \quad (6.63)$$

The quality in the ADS4 line is a very critical parameter in the oscillation behavior. Unfortunately, the quality in the ADS4 line is very difficult to determine analytically and due to the importance of the quality in the simulation, a correlation relating ADS4 liquid flow and quality was used. From the data, the following relation was determined.

$$x = \frac{1}{\left[1 + \dot{m}_{ADS4, f, i}^c\right]^b} \quad (6.64)$$

The coefficients were determined by curve fitting data as shown in figure 6.2.

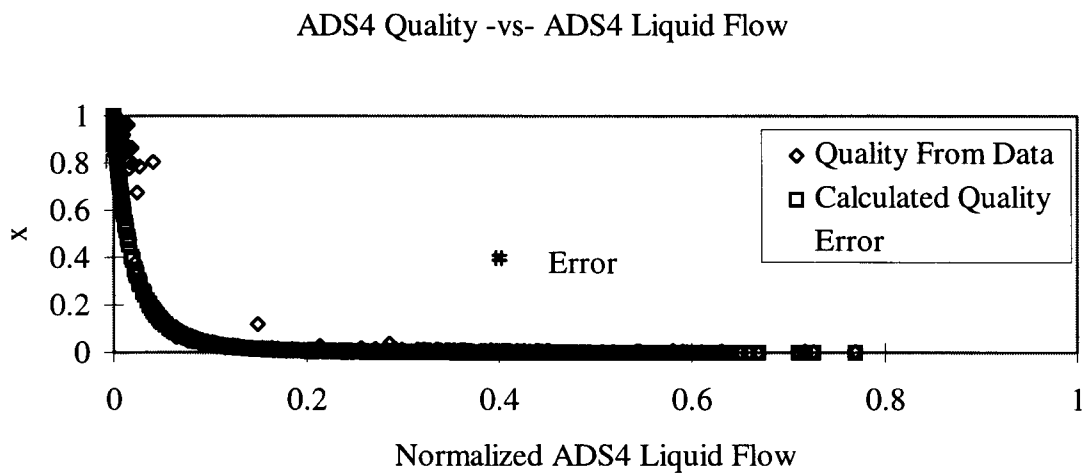


Figure 6.2 Plot showing the quality versus ADS4 liquid flow.

Figure 6.3 is a flow chart of the APOS code. It describes the logical pathway the code takes to calculate the RSO oscillation. The code begins by initializing the system temperatures and flow velocities using the parameters provided in the input section of the spreadsheet. The reactor head pressure is calculated and the fluid flows for all reactor connecting systems are determined using the new head pressure. During this process, the core temperature profiles and steam generation rates are calculated.

Calculated flows are used to determine changes in tank elevations using a conservation of mass approach. Tank levels directly affect the velocities of fluid entering and exiting the system and these parameters are shown in the figure by dashed lines.

A simple logic flag determines whether or not steam is venting from the ADS4 line and the logic to turn on the flag on and off is presented in the figure. If the conditions for termination are met, the code terminates otherwise it proceeds back to the new determination of reactor head pressure.

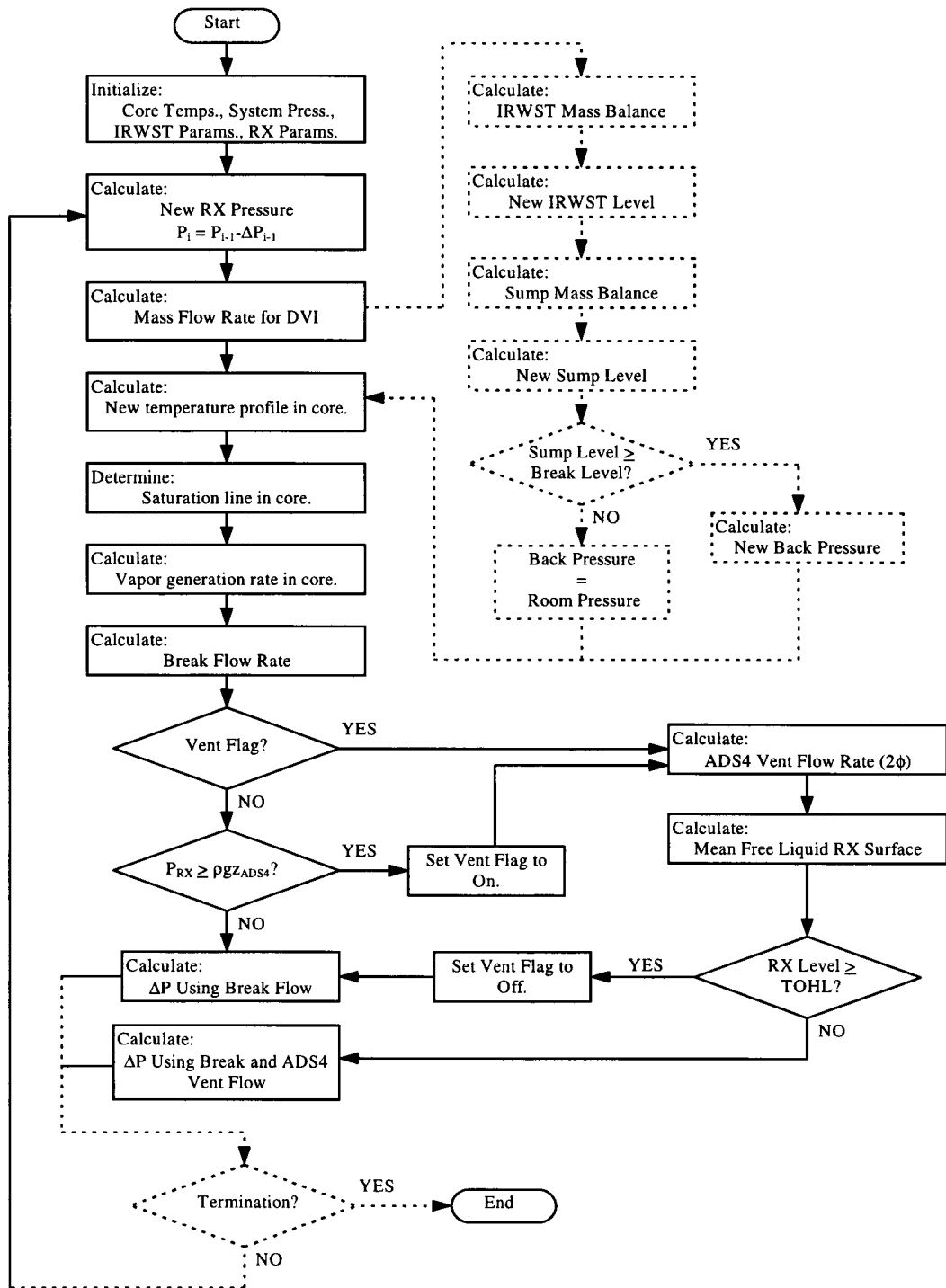


Figure 6.3 Flow chart for the APOS code. Dashed Lines indicate sections of the code which represent changing reactor inputs.

6.5 Onset and Termination

The mechanism for the onset of the oscillations is relatively straight forward. The primary driving parameter of the oscillations is the pressure change in the steam volumes of the primary system. There are two ingredients causing changes in the pressure: steam entering the volumes being created in the bundle and steam venting the system through pathways that change by some mechanism. Both mechanisms are required for oscillations.

The steam pathways in the system always exist (break and ADS 4) and the mechanism causing them to turn on and off requires special conditions in the reactor which typically are present at the point of the return to saturation conditions. It is therefore pertinent to predict when the primary system will return to saturation conditions at the top of the core. This is not very difficult.

Looking at a quasi-steady state approach, the same equations used to develop the DVI flow and equivalently the, core flow can be used. The amount of liquid flowing through the reactor is estimated using equation 6.25 and knowing the amount of power generated in the bundle is known. Therefore it is simple to determine the exit temperature. Using the following relationship

$$q = \dot{m}C_p(T_{out} - T_{in}) \quad (6.65)$$

and applying the following requirements:

$$\dot{m} = \dot{m}_{inject}$$

$$T_{\text{out}} = T_{\text{sat}}$$

it is simple to relate the power required to saturate the core for a given IRWST level using equation 6.24 and equation 6.23.

$$q_{\text{bundle}} = \left[2 \rho \sqrt{\frac{\left[z_{\text{IRWST},i} - z_{\text{RX},i} - \frac{P_{\text{RX},i}}{\rho g} \right] 2 g}{1 + k_{\text{DVI}}} \frac{\pi D_{\text{DVI}}^2}{4} - \dot{m}_{\text{break}}} \right] C_p (T_{\text{sat}} - T_{\text{inject}}) \quad (6.66)$$

Non-dimensionalizing this equation can be done by making the following division to both sides,

$$\frac{q_{\text{bundle}}}{C_p (T_{\text{sat}} - T_{\text{inject}})} = 2 \rho \sqrt{\frac{\left[z_{\text{IRWST},i} - z_{\text{RX},i} - \frac{P_{\text{RX},i}}{\rho g} \right] 2 g}{1 + k_{\text{DVI}}} \frac{\pi D_{\text{DVI}}^2}{4} - \dot{m}_{\text{break}}}, \quad (6.67)$$

and dividing both sides by an initial velocity at the time the IRWST is full ($z_{\text{IRWST},0}$) and simplifying,

$$\frac{q_{\text{bundle}}}{2 \rho \frac{\pi D_{\text{DVI}}^2}{4} C_p (T_{\text{sat}} - T_{\text{inject}})} + \frac{\dot{m}_{\text{break}}}{2 \rho \frac{\pi D_{\text{DVI}}^2}{4} \sqrt{\frac{\left[z_{\text{IRWST},0} - z_{\text{RX},i} - \frac{P_{\text{RX},i}}{\rho g} \right] 2 g}{1 + k_{\text{DVI}}}}} = \frac{\sqrt{\frac{\left[z_{\text{IRWST},i} - z_{\text{RX},i} - \frac{P_{\text{RX},i}}{\rho g} \right] 2 g}{1 + k_{\text{DVI}}}}}{\sqrt{\frac{\left[z_{\text{IRWST},0} - z_{\text{RX},i} - \frac{P_{\text{RX},i}}{\rho g} \right] 2 g}{1 + k_{\text{DVI}}}}}, \quad (6.68)$$

yields a non-dimensional expression for the onset time.

The termination of the oscillations occurs when several conditions are met at the same time. The main key for one oscillation to lead to another is the sealing of the ADS 4 by the mean free liquid surface in the reactor vessel. This occurs because the amount of liquid being pulled from the reactor by the two-phase flow in the ADS 4 train is less than the amount of liquid entering the reactor through the DVI at the minimum pressure point of the oscillation. If the mass flow of the liquid exiting the reactor were to equal the mass flow of liquid entering the reactor, the mean free liquid surface in the reactor would never re-seal the ADS 4 train and the oscillations would terminate.

It is believed that this is the scenario that takes place to terminate the oscillations. This occurs at a particular time due to the transient nature of the DVI flow. The driving head of the DVI flow gradually drops because the liquid level in the IRWST is falling.

In order to quantify this artifact, it is possible to again relate the IRWST level to the core power. The mass flow for the liquid into the reactor is determined using the same relationship as for onset. The amount of liquid leaving the reactor is calculated by using equation 6.60 and resolving the liquid flow entrained in that mass flow. Using equation 6.62, we can link DVI injection flow to liquid flow rate out the ADS 4 line.

If we require the mass flow rate of liquid out ADS 4 to equal DVI injection mass flow using equation 6.24, we can determine how much steam is needed to entrain the injection liquid. First we solve for m_f in equation 6.62 and set it equal equation to 6.24 making the substitutions in 6.23.

$$\frac{\dot{m}_g (1 - x_{\text{ADS4}})}{x_{\text{ADS4}}} = 2 \rho \sqrt{\frac{\left[z_{\text{IRWST},i} - z_{\text{RX},i} - \frac{P_{\text{RX},i}}{\rho g} \right] 2g}{1 + k_{\text{DVI}}} \frac{\pi D_{\text{DVI}}^2}{4} - \dot{m}_{\text{break}}} \quad (6.69)$$

Then relating the mass flow rate of vapor using equations 6.43 and 6.37, the connection between reactor power and IRWST level can be seen.

$$\frac{9.33 q'_{\text{avg},i} L \left[\frac{\left(1 - \frac{z_{\text{sat}}}{L}\right)^{\frac{4}{3}}}{4} - \frac{\left(1 - \frac{z_{\text{sat}}}{L}\right)^{\frac{7}{3}}}{7} \right]}{h_{\text{fg}}} = \left[2 \rho \sqrt{\frac{\left[z_{\text{IRWST},i} - z_{\text{RX},i} - \frac{P_{\text{RX},i}}{\rho g} \right] 2g}{1 + k_{\text{DVI}}} \frac{\pi D_{\text{DVI}}^2}{4} - \dot{m}_{\text{break}}} \right] \frac{x_{\text{ADS4}}}{(1 - x_{\text{ADS4}})} \quad (6.70)$$

Solving for core power as a function of IRWST reactor level provides the desired relation.

$$q_{\text{bundle}} = \frac{\left[2 \rho \sqrt{\frac{\left[z_{\text{IRWST},i} - z_{\text{RX},i} - \frac{P_{\text{RX},i}}{\rho g} \right] 2g}{1 + k_{\text{DVI}}} \frac{\pi D_{\text{DVI}}^2}{4} - \dot{m}_{\text{break}}} \right] \frac{x_{\text{ADS4}}}{(1 - x_{\text{ADS4}})} h_{\text{fg}}}{9.33 \left[\frac{\left(1 - \frac{z_{\text{sat}}}{L}\right)^{\frac{4}{3}}}{4} - \frac{\left(1 - \frac{z_{\text{sat}}}{L}\right)^{\frac{7}{3}}}{7} \right]} \quad (6.71)$$

Equation 6.71 describes termination when the system is at the low pressure of the oscillations. It is desirable to non-dimensionalize this expression using the same steps

for the onset relationship. This leads to the final expression.

$$\begin{aligned}
 & 9.33 \left[\frac{\left(1 - \frac{z_{\text{sat}}}{L}\right)^{\frac{4}{3}}}{4} - \frac{\left(1 - \frac{z_{\text{sat}}}{L}\right)^{\frac{7}{3}}}{7} \right] q_{\text{bundle}} \\
 & \frac{\dot{m}_{\text{break}}}{\left[2\rho \sqrt{\frac{z_{\text{IRWST},0} - z_{\text{RX},i} - \frac{P_{\text{RX},i}}{\rho g}}{1+k_{\text{DVI}}}} \right] \frac{\pi D_{\text{DVI}}^2}{4} \frac{x_{\text{ADS4}}}{(1-x_{\text{ADS4}})} h_{\text{fg}} \left[2\rho \sqrt{\frac{z_{\text{IRWST},0} - z_{\text{RX},i} - \frac{P_{\text{RX},i}}{\rho g}}{1+k_{\text{DVI}}}} \right] \frac{\pi D_{\text{DVI}}^2}{4}} \\
 & = \\
 & \frac{\sqrt{\left[z_{\text{IRWST},i} - z_{\text{RX},i} - \frac{P_{\text{RX},i}}{\rho g} \right]}}{\sqrt{\left[z_{\text{IRWST},0} - z_{\text{RX},i} - \frac{P_{\text{RX},i}}{\rho g} \right]}}
 \end{aligned}$$

(6.72)

7. Comparisons of the APOS code with APEX plant data.

7.1 Introduction

Because of the proprietary concern for data taken at the APEX test facility, the X axis and Y axis have been normalized on the plots and the zero time shifted. The normalizations of the Y axis were done by picking a specific value for each parameter and dividing all the Y data by that value. It would be possible to reconstruct the actual values for the Y axis if the initial number was known however, proprietary concerns require the axis to be normalized. The plots in this chapter will compare results obtained using the APOS code and data collected at the APEX test facility. This chapter will also discuss the NRC-13 series of test which were performed at the APEX testing facility.

7.2 The NRC-13 test series

The objective of the NRC-13 series of tests was to obtain a better understanding of the RSO behavior (10). Several of the external parameters to the primary system were removed by isolation. These parameters included the accumulators, the core makeup tanks, the primary residual heat removal heat exchanger, and the sump. The majority of these components were isolated from the primary with exception to the sump. The sump was drained to ensure the level would not interfere with any of the exit flows of the system.

The primary goal was to induce RSO and then observe the behavior with steady state inputs into the primary system. The APEX plant was brought up to steady state conditions about 10% above atmospheric saturated conditions. The plant was then allowed to blow down using the break valves and the ADS4 lines. The IRWST was allowed to drain from a full tank until the oscillations began. Power to the reactor was held steady.

When the RSO began, the level in the IRWST was held steady by adding water through a throttle valve and maintaining the mass of water in the tank using a load cell beneath the tank. The oscillations were allowed to continue for roughly ten minutes and the IRWST tank elevation was dropped approximately 4% before another ten minute steady state reading was taken. This continued until the RSO terminated. After termination had occurred, the power was dropped approximately 10% to reintroduce conditions for RSO onset. Figure 7.1 shows three RSO onsets that were obtained during the second NRC-13 test. This figure shows the three periods of oscillations separated by two periods where the oscillations have terminated because of reduced IRWST level. The oscillations were restarted by decreasing the core power.

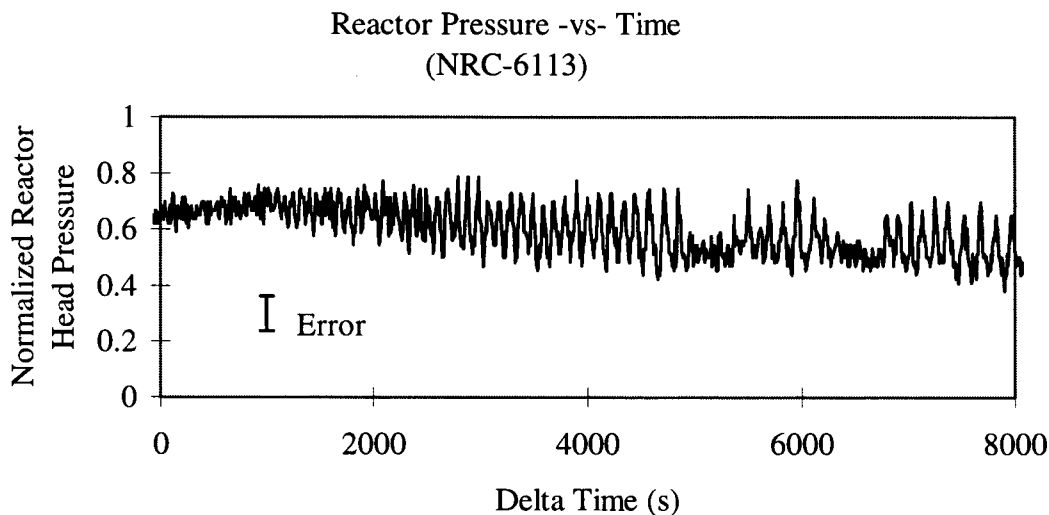


Figure 7.1 Plot showing the three RSO onsets for the NRC-6113 test.

There were three NRC-13 tests performed at the APEX facility. The first test was very successful capturing three RSO onsets and providing solid steady state data. The second test was performed with new instrumentation installed in the plant. This new instrumentation was necessary to capture steam flows leaving the plant. Prior data showed no steam leaving the plant due to the ranging of the steam vortex meters in the facility. After installing more sensitive instrumentation in parallel vent lines, the steam from the primary plant was rerouted to these instruments after the initial plant blowdown.

Unfortunately the new instruments showed very little steam leaving the plant during the oscillations and analysis showed the energy entering and leaving the system could be tracked almost completely using liquid inventories, liquid flows into and out of the system, and core power. Because of the lack of instrumentation inside the reactor itself, boiling profiles and two-phase behavior in the primary plant is very difficult to

understand. The instrumentation on the ADS4 separators is also incapable of providing clear flow behavior during the RSO.

Due to these problems, a third test was performed. Clear piping was installed in the ADS4 lines in order to physically observe the ADS4 flow behavior. Even though the APEX instrumentation shows the ADS4 flow going almost to zero, photographic evidence proves the flow goes to zero for almost half of the oscillation as shown in Figure 7.2. Two-phase flow is also observed proving that steam is flowing through that line and that the instrumentation is not indicative for predicting the behavior in the plant.



Figure 7.2 Photo showing the ADS4 piping during the RSO.

7.3 NRC Data Comparisons

This is a short section showing code comparisons to actual APEX test data in Figures 7.3 through 7.9. The data shown is a typical break scenario in the plant where oscillations can be observed. The parameters of pressure, IRWST level, core power, DVI flow, axial core temperatures, RX mean free surface, and ADS4 liquid flows are all critical parameters concerning the behavior of the RSO. The following figures show how closely the code and actual data compare.

Figure 7.3 shows the APOS predictions of reactor head pressure agree well with the data. This supports the use of the perfect gas law for pressure estimates. Note the increasing pressure amplitudes with time.

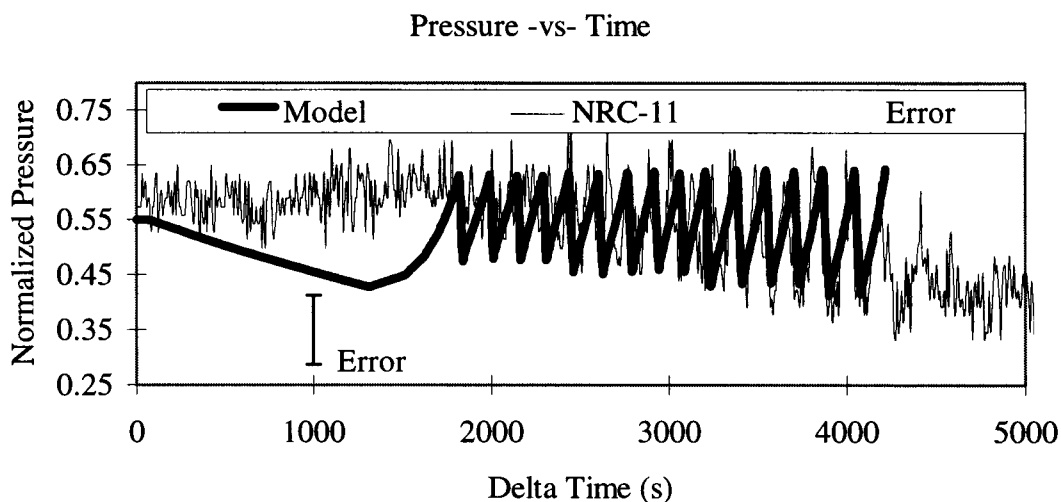


Figure 7.3 Plot showing APOS code results to actual APEX data for pressure.

Figure 7.4 shows the Bernoulli equations adequately predicts the DVI flow and the line resistances are adequately modeled.

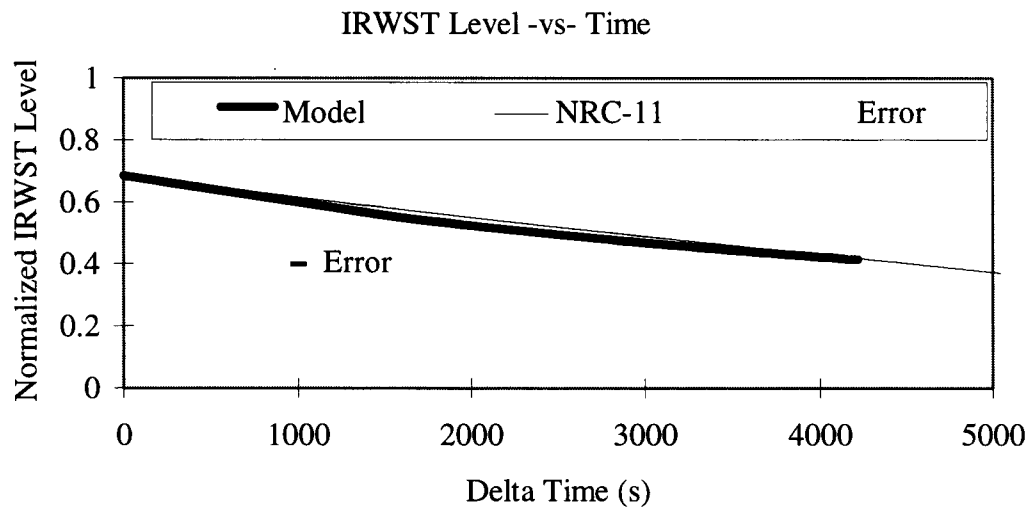


Figure 7.4 Plot showing APOS code results to actual APEX data for IRWST Level.

Good comparison between APOS and data can be seen in Figure 7.5 because power is an input parameter for both the test and the code.

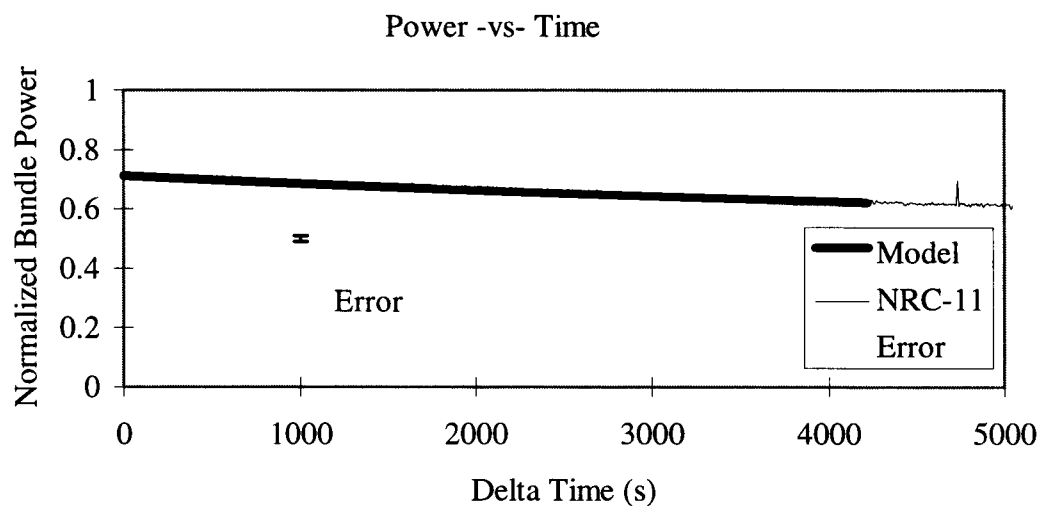


Figure 7.5 Plot showing APOS code results to actual APEX data for core power.

Figure 7.6 shows DVI flow falling off to zero later in the RSO. This behavior is not seen in test data but is seen during the flow visualization tests.

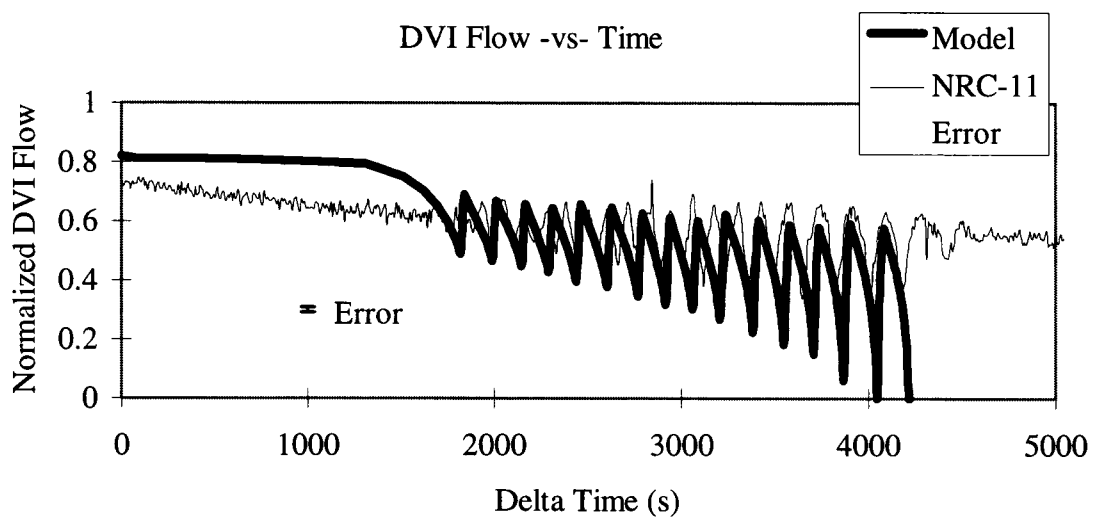


Figure 7.6 Plot showing APOS code results to actual APEX data for DVI Flow.

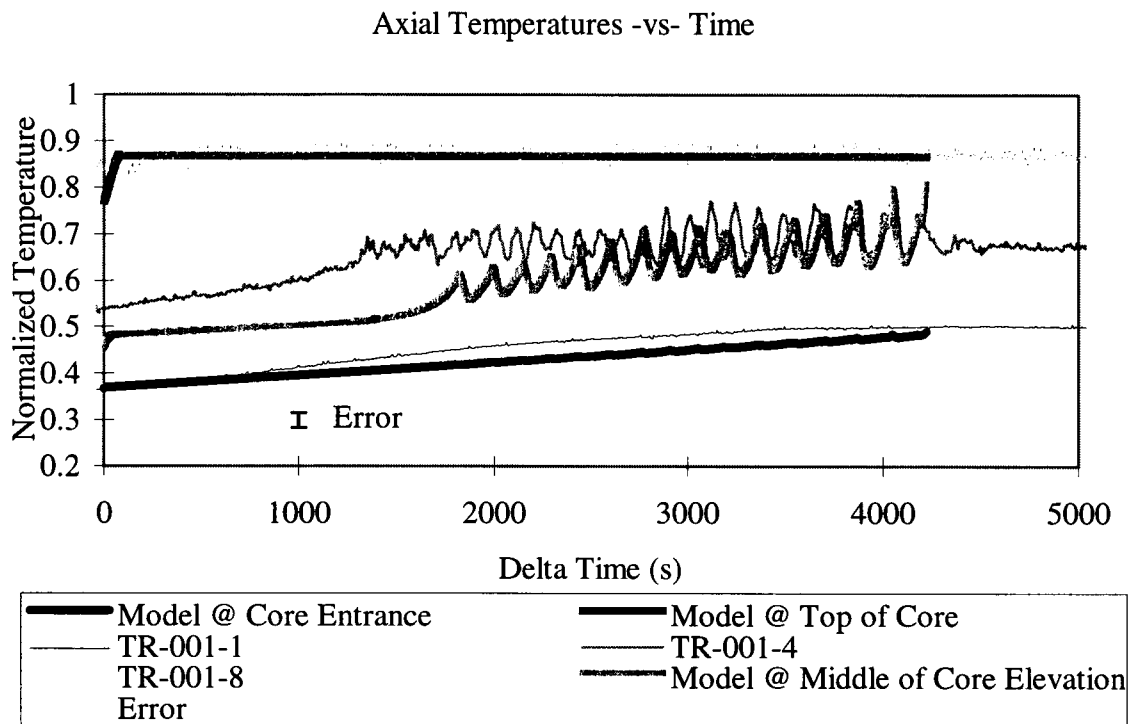


Figure 7.7 Plot showing APOS code results to actual APEX data for core temperatures.

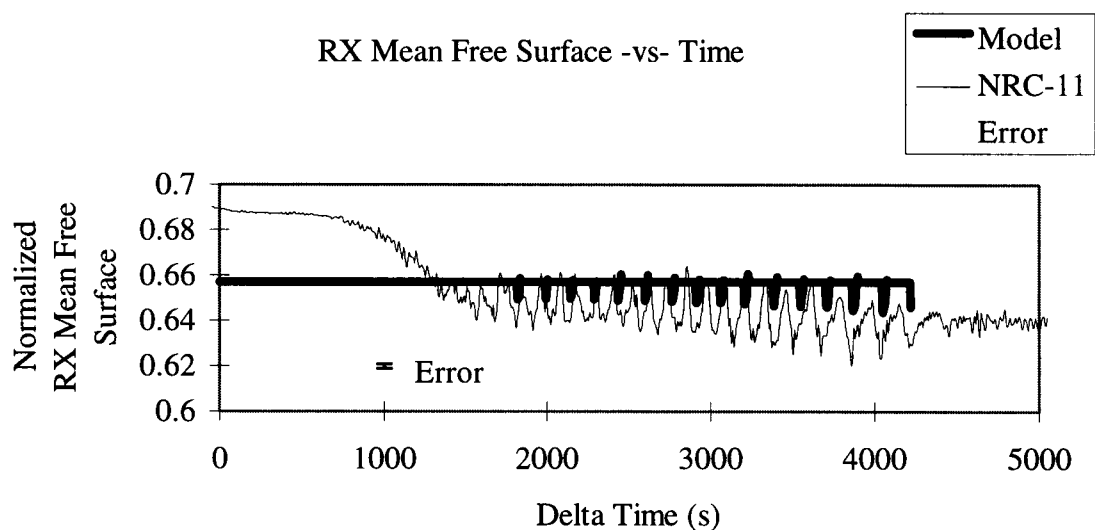


Figure 7.8 Plot showing APOS code results to actual APEX data for the RX mean free surface.

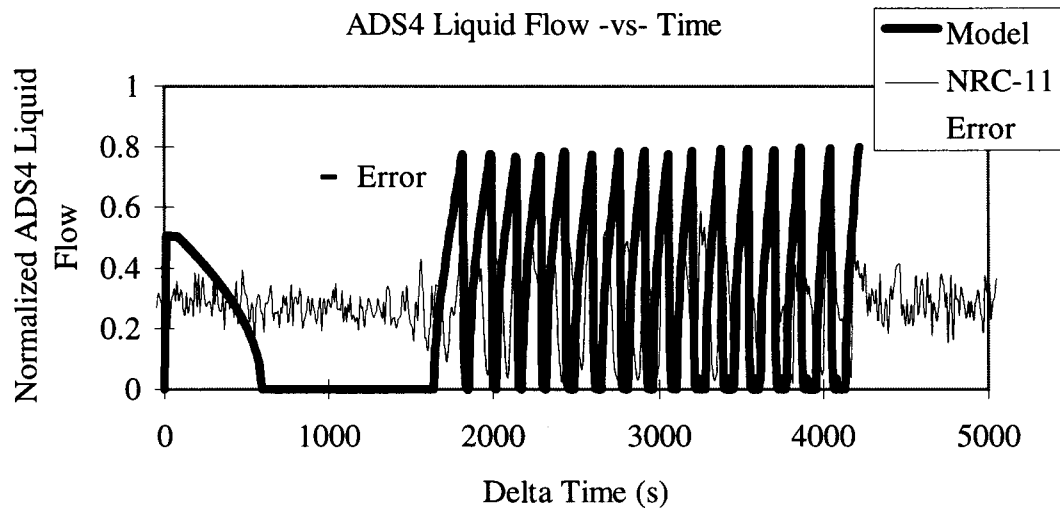


Figure 7.9 Plot showing APOS code results to actual APEX data for ADS4 liquid flows.

7.4 Conclusions

From the comparisons of data to model, I can say there is good understanding of how the RSO works.

8. Scaling to the actual AP600

8.1 Introduction

Scaling the RSO to the full size AP600 would be of great interest to both the designers and the NRC. Scaling this particular phenomenon is very difficult. Aspects of the phenomenon may be impossible to scale with the current level of understanding.

8.2 Oscillation characteristics which can be scaled

Of the five characteristics which are described in chapter five, not many are very scaleable to the full scale plant. In actuality, our level of understanding of the RSO is such that dimensionless parameters become very difficult to construct for scaling analysis. Of the parameters that can be scaled, onset seems to be the easiest. Formulas for the onset criteria have been stated earlier and these formulas can be used for predicting onset behavior in the real plant.

The amplitude of the oscillation is also relatively straight forward to predict using the known containment pressure and plant geometry. Knowing that the APEX test facility is a 1/4 scale model, the amplitude is expected to be four times as large in the AP600 due to the ADS4 line being four times taller. The following equation expresses this relationship.

$$Z_{\text{APEX}} = \frac{Z_{\text{AP600}}}{4} \quad (8.1)$$

and since

$$P = \rho gz \quad (8.2)$$

it is possible to multiply both sides of this equation by ρg and arrive at the following result.

$$4 \times P_{\text{APEX}} = P_{\text{AP600}} \quad (8.3)$$

From this we can calculate the pressure amplitude of the AP600 oscillation wave.

8.3 Oscillation characteristics which make scaling very difficult

The termination mechanism for the oscillations is very difficult to scale for several reasons. The most prominent reason includes the two-phase behavior of the ADS4 line. Top offtake flow behavior is not well understood nor well mapped in test data. Due to the venting behavior the ADS4 line contributes to the RSO, termination and period are both very difficult to model.

The core power profile also makes it difficult to predict core recirculation patterns and the potential condensation effects those patterns may induce. With the venting behavior of the plant being sketchy, it's also difficult to determine the period of the oscillations.

Three things make a full scaled simulation by APOS inaccurate; an accurate model for vapor quality for vertical offtakes is not available, termination is difficult to determine, and the period cannot be scaled because condensation effects within the full scaled facility are unknown.

9. Conclusions and Summary

9.1 General Overview

The following research tasks have been covered and explained in the paper.

- Existing RSO data has been collected and studied.
- A computer model (APOS) was developed to simulate the oscillation behavior.
- A set of steady state tests (NRC-13) which were designed to study the RSO directly were successfully performed at the APEX testing facility. The testing included flow visualization in the ADS4 line.

The following findings were made.

- Key stages of the oscillation were identified.
- The RSO does not lead to the threat of core uncovering.
- Close agreement of the APOS model and actual data proves the RSO is well understood in the APEX facility.
- Scaling of onset and amplitude of the RSO is possible to the full scale facility.
- Scaling of termination and period to the full scale facility were found to be difficult due to unknown characteristics of the ADS4 two-phase flows and reactor recirculation patterns.

Several key features for future work were identified.

- Better correlations for two-phase flow for a vertical offtake need to be developed.

- The effects of the power profile on steam generation and core recirculation patterns are unknown. Work in this area would be useful.
- A better set of instrumentation in the reactor would be useful in the future.

Oregon State University has built a testing facility for the purpose of investigating the safety systems of a new nuclear power plant design, AP600. During the operation of the testing facility, a phenomenon called the Return to Saturation Oscillations (RSO) was observed for several tests. Because of the safety concern this phenomenon could pose, a more in depth study was performed.

The RSO phenomenon was observed for scaled two inch break scenarios in the facility. The general sequence of events for a test consisted of a blowdown period which brought the pressure of the primary system close to atmospheric pressure. When the low primary pressure is reached, cold liquid can flow by gravity into the primary system from the large IRWST tank. When the tank is full, the driving head is large enough to subcool the reactor region of the core, but as the tank drains, the driving head slowly decreases.

Eventually the flow from the IRWST drops low enough to allow the exit of the core to become saturated and steam generation in the primary begins. This is the point of return to saturation and the onset of the oscillations; hence the name, "Return to Saturation Oscillations." To better understand the oscillation behavior, several tasks were carried out.

The first task was to collect and study data which had already been acquired at the facility. The next task was to build a computer model to simulate the oscillations. The code was constructed using plant geometry, core power and material parameters.

The code uses a simple mass and energy balance approach for node analysis. Flows from one node to another are calculated using mass conservation and Bernoulli's equation. A modified perfect gas law approach is used to determine pressure changes in the reactor head.

Another task consisted of performing particular tests which were targeted at better defining the RSO behavior. The NRC-13 series of tests were conducted with many of the primary system components (CMT's, ACC's, PRHR, Sump) isolated and drained to reduce the number of parameters which may affect the RSO behavior. The objective of the tests was to induce oscillation behavior, obtain steady state data for a reasonable period and observe termination. The test objectives were met with great success and physical observations of the phenomenon were obtained.

In general, the phenomenon is well understood in the APEX facility.

9.2 Safety and Scaling Issues

Of the issues associated with this phenomenon, safety and scaling are paramount. It is not difficult to state that the phenomenon does not pose a safety concern. From the designers viewpoint, core uncovering is the chief concern. This particular phenomenon does not introduce factors which would contribute to a situation causing core uncovering. The critical factor for the phenomenon concerns the cessation of injection flows. When the liquid inventory in the reactor drops to an elevation equal to or near the top of the hot leg, steam venting begins which lowers reactor head pressure and injection flows start again posing no threat to core uncovering.

Naturally we would like to be able to predict this behavior in the real plant. A model which could be added to existing codes for behavior prediction can be very useful not only to the primary system behavior but for the relationships with other system components. Unfortunately our understanding of the phenomenon makes a prediction extremely difficult due to the lack of understanding of two-phase phenomenon particularly for a vertical offtake on a pipe and the lack of instrumentation in the reactor vessel itself.

A clear picture of the fluid circulation patterns with the reactor vessel during the oscillations is very sketchy at best. RSO onset and the amplitude of the oscillation can be predicted but termination and period are unclear at the moment. Differences in the power profile used at the APEX facility versus the real plant and certain geometrical factors make termination and period very difficult to predict for a full scale application. Indeed these factors make it difficult to even say RSO will occur in the full scale facility. This makes our understanding of this phenomenon confined to the APEX facility.

9.3 Roadmap for future work

During this work, several things were found which could have made the analysis more complete. Correlations and data concerning the behavior of two-phase flow for a top offtake on a pipe would have made the behavior easier to predict. If this type of data existed over a wide range of geometries and fluid conditions, prediction of particular parameters for the full scale facility would be easier.

The effects of the power profile in the APEX existing facility versus the real plant would also be very interesting and critical for a good prediction of the RSO behavior in the actual plant. A better set of instrumentation in the APEX facility may have been good for better understanding of the behavior in the primary particularly in the core region. A better set of thermocouple rakes could be installed into the core region and potentially some types of instruments could be installed which could describe void fraction and swelled liquid levels. Flow patterns and temperature profiles for this part of the reactor are very sketchy.

Bibliography

1. Westinghouse Electric corp. AP600 Standard Safety Analysis Report, Westinghouse Electric Corp. Pittsburgh Penn., 1992.
2. Westinghouse Electric corp. AP600 Low Pressure Integral Systems Test at Oregon State University Facility Description Report, Westinghouse Electric Corporation, Pittsburgh Penn, 1994.
3. Hsu, Yih-Yun, Graham, Robert W., Transport Processes in Boiling and Two-Phase Systems, 1976, Hemisphere Publishing Corporation, Washington, London
4. G.B. Wallis, J.H. Heasley, Oscillation in Two-phase Flow Systems, J. Heat Transfer, 83C(3), 363-369, 1961
5. Maulbetsch, J. S., Griffith, P., System-Induced Instabilities in Forced-Convection Flows with Subcooled Boiling, 1966, Proc. 3rd Int. Heat Trans. Conf., AIChE, Vol 4, PP 247-257
6. Jain, K.C., Petrick, M., Miller, D., Bankoff, S.G., Self-Sustained Hydrodynamic Oscillations in a Natural-Circulation Boiling Water Loop, 1966, Nuclear Engineering and Design 4, North-Holland Publishing Company, Amsterdam.
7. Davis, A. Douglas, Classical Mechanics, 1986, Academic Press, Orlando Florida.
8. N. Zuber, Flow Excursion and Oscillations in Boiling, Two-Phase Flow System with Heat Addition, International Symposium on Two-Phase Flow Dynamics, The Netherlands, 1967.
9. Lamb, Sir Horace, Hydrodynamics, 1993, Cambridge University Press, New York, New York., PP 311-325
10. APEX Testing Facility, NRC-13 Quick Look Report, Corvallis OR, Oregon State University, 1995.
11. APEX Testing Facility, NRC-11 Quick Look Report, Corvallis OR, Oregon State University, 1995.
12. APEX Testing Facility, SB-15 Quick Look Report, Westinghouse Electric Corporation, Pittsburgh Penn, 1994.
13. Microsoft, Excel Version 7.0, Seattle Wa, 1995.
14. Westinghouse, Quick Look Report for the Flow Test/Line Resistnace Determination, Westinghouse Electric Corp., Pittsburgh Penn, 1994,

15. Reyes Jr., Dr. Jose N., Low-Pressure Integral Systems Test Facility Scaling Report, Jan 1995, Westinghouse Electric Corporation, Pittsburgh Pennsylvania., 1994
16. Welty, James R., Wicks, Charles E., and Wilson, Robert E., Fundamentals of Momentum, Heat and Mass Transfer, Third Edition, John Wiley & Sons, 1984.
17. Serway, Raymond, Physics for Scientists and Engineers with Modern Physics, 1986, Saunders College Publishing, Philadelphia, New York, Chicago, San Francisco, Montreal, Toronto, London, Sydney, Tokyo, Mexico City, Rio de Janeiro, Madrid

Appendix
APOS Code Listing

Sub APOS()

'This code is designed to simulate the Return to Saturation oscillations seen in the APEX test facility.

'First initialize the calculation

Dim RowNum, RXPress, IRWSTZ, SumpZ, Power, RXz, DVIRho, DVlk, Gravity, Pi, DVIA, _
 Term1, DVlmdot, DVlv, Tinject, qnode, Nodez, Halfz, L, j, i, Cpf, Mnode, TOutnit, _
 DeltaTemp, qPavg, Deltaz, DeltaTNode, Tnew, Tsat, Count, zSat, qSteam, BreakRho, _
 ABreak, BreakMDot, SumpPress, Breakk, VentFlag, TimeStep, R, SteamV, hfg, SteamMDot, _
 DeltaP, AIRWST, OldTemp, NewTemp, Cvf, TempBelow, ADS4MDot, ADS4k, x, TPRho, AADS4, _
 ADS4v, RXA, OldRXz, NewRXz, ADS4Fric, ADS4z, TOHL, Maxlter, PDA, PDB, SimTime, _
 PlantTime, StartTime, EndTime, CalcTime, lterTime, Trigger, QTtotal, ADS4Total, _
 BreakTotal, DVITotal, SumQ, xStep, lterDirection, hfsat, hgsat, AbsSumQ, _
 Update, vlg, vl, vg, First, Relativek

' Feb 10, 1997

' We're going to rework the break logic here. We're going to make the break a solid liquid
 ' vent pathway and call breakmdot the amount of steam that was condensed in the break liquid.
 ' We're going to call the amount of liquid that left the break.
 ' We're going to cook up a number to multiply BreakMLiq with to determine breakmdot.
 ' We're going to introduce the RPSGCF (Radial Profile Steam Generation Correction Factor)
 ' The RPSGCF will be multiplied with the steam generation rate to reduce the amount of steam
 ' produced in the core. Hopefully, the oscillations that this version has been able to produce
 ' so far will continue. We're also going to introduce another factor with which the amount of steam
 ' condensed in the downcomer can be turned on and off wrt the core depression rate.
 ' Tonight I've already implemented the IRWST injection incline temperature and a termination
 ' cutoff which seems to work just fine.

Pi = 3.1415927

RowNum = 20

Trigger = 0

First = 1

Windows("MODCOD6B.XLS").Activate

Sheets(1).Activate

With Application

.Calculation = xlManual

.MaxChange = 0.001

End With

Range("A21:AP3020").Select

Selection.Clear

Range("D19:E19").Select

Selection.NumberFormat = "h:mm:ss"

Range("A20:A20").Select

Calculate

' Sheets(16).Activate

i = 1

Sheets(1).Cells(19, 5) = Empty

TimeStep = Sheets(1).Cells(9, 2)

CondFrac = Sheets(1).Cells(7, 9)

RPSGCF = Sheets(1).Cells(3, 8)

BreakThresh = Sheets(1).Cells(11, 8)

StartTime = Time

IRWSTSlope = Sheets(1).Cells(13, 8)

IRWSTInter = Sheets(1).Cells(14, 8)

Terminal = Sheets(1).Cells(17, 8)

```

hfsat = Sheets(1).Cells(1, 17)
hgsat = Sheets(1).Cells(2, 17)
hfdvi = Sheets(1).Cells(3, 17)
PlantTime = Sheets(1).Cells(8, 8)
Sheets(1).Cells(18, 2) = Time
PDA = Sheets(1).Cells(5, 8)
Sheets(1).Cells(19, 6) = "In Progress"
PDB = Sheets(1).Cells(6, 8)
MaxIter = Sheets(1).Cells(2, 7)
Sheets(1).Cells(19, 2) = Empty
x = Sheets(1).Cells(16, 6)
ADS4Fric = Sheets(1).Cells(17, 6)
ADS4z = Sheets(1).Cells(10, 2)
ADS4k = Sheets(1).Cells(12, 2)
AADS4 = Pi * Sheets(1).Cells(13, 6) ^ 2 / 4
RXA = Pi * Sheets(1).Cells(11, 6) ^ 2 / 4
RXPress = Sheets(1).Cells(8, 6)
Sheets(1).Cells(i + RowNum, 3) = RXPress / 144
IRWSTZ = Sheets(1).Cells(6, 6)
Sheets(1).Cells(i + RowNum, 4) = IRWSTZ * 12 - 106.99
RXz = Sheets(1).Cells(7, 6)
TOHL = RXz
Gravity = Sheets(1).Cells(8, 2)
DVIRho = Sheets(1).Cells(5, 4)
DVIk = Sheets(1).Cells(6, 2)
DVIA = Pi * Sheets(1).Cells(5, 6) ^ 2 / 4
Term1 = ((IRWSTZ - RXz - (RXPress / DVIRho)) * 2 * Gravity) / (1 + DVIk)
If Term1 <= 0 Then DVlv = 0 Else DVlv = Sqr(Term1)
DVImdot = DVIRho * DVIA * DVlv * 2
Sheets(1).Cells(i + RowNum, 6) = DVImdot * 60 / DVIRho * 7.4805

' Perform IRWST Injection Temp
Tinject = IRWSTInter

Cpf = Sheets(1).Cells(6, 4)
Cvf = Cpf
L = Sheets(1).Cells(8, 12)
AIRWST = Sheets(1).Cells(15, 6) ^ 2 / 4 * Pi

' Initialize the core node temperatures
Sheets(1).Cells(i + RowNum, 8) = Tinject
Mnode = Sheets(1).Cells(16, 11)
TOutlnit = Power / (DVImdot * Cpf) + Tinject
DeltaTemp = TOutlnit - Tinject
SimTime = i * TimeStep + PlantTime
Power = 600 / (1 + PDA * (SimTime - 140)) ^ PDB * 3412 / 3600
Sheets(1).Cells(i + RowNum, 5) = Power * 3600 / 3412
qPavg = Power / L
Deltaz = Sheets(1).Cells(14, 11)
Halfz = Deltaz / 2
Tsat = Sheets(1).Cells(10, 4)
j = 1
Do Until j = 20
  j = j + 1
  Nodez = j * Deltaz - Halfz
  qnode = 3.11 * qPavg * (Nodez / L) * (1 - (Nodez / L)) ^ (1 / 3) * Deltaz

```

```

DeltaTNode = qnode / (DVImdot * Cpf)
Tnew = Sheets(1).Cells(i + RowNum, j + 6) + DeltaTNode
If Tnew > Tsat Then Tnew = Tsat
Sheets(1).Cells(i + RowNum, j + 7) = Tnew
Loop
'Determine the saturation line elevation
j = 0
Count = 0
Do Until j = 20
  j = j + 1
  If Sheets(1).Cells(i + RowNum, j + 7) = Tsat Then Count = Count + 1
Loop
zSat = L - Count * Deltaz
Sheets(1).Cells(i + RowNum, 28) = zSat * 12
qSteam = 9.33 * qPavg * L * (((1 - zSat / L) ^ (4 / 3) / 4) - ((1 - zSat / L) ^ (7 / 3) / 7))
Sheets(1).Cells(i + RowNum, 29) = qSteam

' Initialize the rest of the data
ABreak = Pi * Sheets(1).Cells(12, 6) ^ 2 / 4
BreakRho = Sheets(1).Cells(7, 4)
SumpPress = 0
Breakk = 1

'Changes Feb 10
' BreakMDot = BreakRho * ABreak * Sqr(2 * Gravity * (RXPress - SumpPress) / (BreakRho * (1 + Breakk)))
BreakMLiq = DVIRho * ABreak * Sqr(2 * Gravity * (RXPress - SumpPress) / (DVIRho * (1 + Breakk)))
BreakMDot = CondFrac * BreakMLiq

If Tnew < Tsat Then BreakMDot = 0
Sheets(1).Cells(i + RowNum, 30) = BreakMDot

VentFlag = 0
Sheets(1).Cells(i + RowNum, 32) = RXz * 12 - 40.89
R = Sheets(1).Cells(11, 4)
SteamV = Sheets(1).Cells(16, 2)
hfg = Sheets(1).Cells(9, 4)
SteamMDot = qSteam / hfg
Sheets(1).Cells(i + RowNum, 34) = SteamMDot
DeltaP = TimeStep * (SteamMDot - BreakMDot) * (R * (Tsat + 459.67) / SteamV)
Sheets(1).Cells(i + RowNum, 33) = DeltaP / 144
Sheets(1).Cells(i + RowNum, 1) = i
Sheets(1).Cells(i + RowNum, 2) = PlantTime
Sheets(1).Cells(RowNum + i, 35) = DVImdot
Sheets(1).Cells(i + RowNum, 39) = 0
Update = 0

TPRho = 1 / ((x / BreakRho) + ((1 - x) / DVIRho))
vg = 1 / BreakRho
vl = 1 / DVIRho
vlg = vg - vl
Termination = 0

' Begin the simulation
Do Until i = MaxIter
  i = i + 1
  Update = Update + 1

```

```

CalcTime = Time - StartTime
IterTime = CalcTime / i
EndTime = StartTime + MaxIter * IterTime
Sheets(1).Cells(19, 2) = EndTime
Sheets(1).Cells(19, 4) = EndTime - Time
Sheets(1).Cells(19, 3) = 100 * (MaxIter - i) / MaxIter
Sheets(1).Cells(i + RowNum, 1) = i
Sheets(1).Cells(i + RowNum, 2) = (i - 1) * TimeStep + PlantTime
RXPress = RXPress + DeltaP
Sheets(1).Cells(i + RowNum, 3) = RXPress / 144
'Calculate New IRWST Injection Temp
Tinject = IRWSTSlope * (i * TimeStep) + IRWSTInter
'Calculate New IRWST level
IRWSTZ = IRWSTZ - DVImdot * TimeStep / (DVIRho * AIRWST)
Sheets(1).Cells(i + RowNum, 4) = IRWSTZ * 12 - 106.99
'Calculate DVI Flow
Term1 = ((IRWSTZ - TOHL - (RXPress / DVIRho)) * 2 * Gravity) / (1 + DVlk)
If Term1 <= 0 Then DVlv = 0 Else DVlv = Sqr(Term1)
DVImdot = DVIRho * DVIA * DVlv * 2
Sheets(1).Cells(i + RowNum, 6) = DVImdot * 60 / DVIRho * 7.4805
'Calculate the new power
SimTime = i * TimeStep + PlantTime
Power = 600 / (1 + PDA * (SimTime - 140)) ^ PDB * 3412 / 3600
qPavg = Power / L
Sheets(1).Cells(RowNum + i, 5) = Power * 3600 / 3412
'Calculate Core Temperature Profile
'Do node 1 first
OldTemp = Sheets(1).Cells(i + RowNum - 1, 8)
qnode = 3.11 * qPavg * Deltaz * (Halfz / L) * (1 - Halfz / L) ^ (1 / 3)

' Changes Feb 10, 1997
NewTemp = OldTemp + (TimeStep / (Mnode * Cvf)) * (qnode + ((DVImdot - BreakMLiq) * Cpf * (Tinject - OldTemp)))

If NewTemp > Tsat Then NewTemp = Tsat
Sheets(1).Cells(i + RowNum, 8) = NewTemp
'Do the rest of the nodes.
j = 1
Do Until j = 20
j = j + 1
OldTemp = Sheets(1).Cells(i + RowNum - 1, j + 7)
TempBelow = Sheets(1).Cells(i + RowNum - 1, j + 6)
Nodez = j * Deltaz - Halfz
qnode = 3.11 * qPavg * Deltaz * (Nodez / L) * (1 - Nodez / L) ^ (1 / 3)

' Changes made Feb 10, 1997
NewTemp = OldTemp + (TimeStep / (Mnode * Cvf)) * (qnode + (DVImdot - BreakMLiq) * Cpf * (TempBelow - OldTemp))

If NewTemp > OldTemp + 10 Then Sheets(1).Cells(19, 6) = "Overextended!!"
If NewTemp < OldTemp - 10 Then Sheets(1).Cells(19, 6) = "Overextended!!"
If NewTemp < OldTemp + 10 And NewTemp > OldTemp - 10 Then Sheets(1).Cells(19, 6) = "In Progress"
If NewTemp > Tsat Then NewTemp = Tsat
Sheets(1).Cells(i + RowNum, j + 7) = NewTemp
Loop
'Determine Saturation Line

```

```

j = 0
Count = 0
Do Until j = 20
  j = j + 1
  If Sheets(1).Cells(i + RowNum, j + 7) = Tsat Then Count = Count + 1
Loop
zSat = L - Count * Deltaz
Sheets(1).Cells(i + RowNum, 28) = zSat * 12
'Set initial reactor level condition
If VentFlag = 0 Then RXz = TOHL
'Determine Steam Heat and Steam mass rate
qSteam = 9.33 * qPavg * L * (((1 - zSat / L) ^ (4 / 3) / 4) - ((1 - zSat / L) ^ (7 / 3) / 7))
Sheets(1).Cells(i + RowNum, 29) = qSteam

' Changes Feb 10, 1997
SteamMDot = qSteam / hfg * RPSGCF

  Sheets(1).Cells(i + RowNum, 34) = SteamMDot
'Determine Break Flow Rate

' Changes Feb 10, 1997
BreakMLiq = DVIRho * ABreak * Sqr(2 * Gravity * (RXPress - SumpPress) / (DVIRho * (1 + Breakk)))
If zSat * 12 < BreakThresh Then BreakMLiq = 0
BreakMDot = BreakMLiq * CondFrac

If NewTemp < Tsat Then BreakMDot = 0
Sheets(1).Cells(i + RowNum, 30) = BreakMDot
'Determine ADS 4 Flow Rate
If VentFlag = 0 Then
  TPRho = 1 / ((x / BreakRho) + ((1 - x) / DVIRho))
  Term1 = 2 * Gravity * ((RXPress - SumpPress) / TPRho - ADS4z) / (1 + ADS4k)
  If Term1 <= 0 Then ADS4v = 0 Else ADS4v = Sqr(Term1)
  ADS4MDot = 1.5 * TPRho * ADS4v * AADS4
  Sheets(1).Cells(i + RowNum, 39) = ADS4MDot * 60 / DVIRho * 7.4805
Else
  TPRho = 1 / ((x / BreakRho) + ((1 - x) / DVIRho))
  Term1 = 2 * Gravity * ((RXPress - SumpPress) / TPRho - ADS4z) / (1 + ADS4k)
  If Term1 <= 0 Then ADS4v = 0 Else ADS4v = Sqr(Term1)
  ADS4MDot = 1.5 * TPRho * ADS4v * AADS4
End If
'Calculate the quality
' If VentFlag = 1 And RXPress > 124.4 And RXPress < 172.4 Then _
'   x = 1 / (-0.00062798 * RXPress ^ 3 + 0.306311975 * RXPress ^ 2 - 50.9557 * RXPress + 2907.94)
' If VentFlag = 1 And RXPress >= 172.4 Then x = 0.15
' If VentFlag = 1 And RXPress <= 124.4 Then x = 0.001
  If VentFlag = 1 Then x = 1 / (1 + 0.523991596 * (1 - x) * ADS4MDot) ^ 3.500642507
  If VentFlag = 0 Then x = 0.0001
  If x < 0.0001 Then x = 0.0001
  If x > 1 Then x = 1
'Determine Reactor Elevation
OldRXz = RXz
NewRXz = OldRXz + TimeStep / (DVIRho * RXA) * (DVImdot - (1 - x) * ADS4MDot)
If VentFlag = 1 Then RXz = NewRXz
'Determine Vent Logic
If VentFlag = 0 Then
  If RXPress >= DVIRho * ADS4z + ADS4Fric Then VentFlag = 1

```

```

Else
  If RXz >= TOHL Then VentFlag = 0
End If
'Report to the sheet
  Sheets(1).Cells(i + RowNum, 31) = ADS4MDot
  Sheets(1).Cells(RowNum + i, 32) = RXz * 12 - 40.89
'Determine Delta P
  DeltaP = TimeStep * (SteamMDot - BreakMDot - x * ADS4MDot) * (R * (Tsat + 459.67) / SteamV)
  Sheets(1).Cells(i + RowNum, 33) = DeltaP / 144
'Perform Energy Calculations
  If Trigger = 0 And VentFlag = 1 Then
    Trigger = 1
    Sheets(1).Cells(i + RowNum, 36) = "Trigger"
    QTotal = 0
    ADS4Total = 0
    BreakTotal = 0
    DVITotal = 0
  End If
  If Trigger = 1 And VentFlag = 0 Then Trigger = 0
  QTotal = QTotal + TimeStep * Power
  ADS4Total = ADS4Total + ADS4MDot * TimeStep
  BreakTotal = BreakTotal + BreakMDot * TimeStep
  DVITotal = DVITotal + DVImdot * TimeStep
'Report extras
  Sheets(1).Cells(i + RowNum, 37) = x
  Sheets(1).Cells(i + RowNum, 41) = SteamMDot - BreakMDot - x * ADS4MDot
  Sheets(1).Cells(RowNum + i, 35) = DVImdot - (1 - x) * ADS4MDot
  Sheets(1).Cells(RowNum + i, 38) = (Power + DVImdot * hfdvi - _
  BreakMDot * hgsat - x * ADS4MDot * hgsat - (1 - x) * hfsat * _
  ADS4MDot) * 3600 / 3412
  If RXz <> TOHL Then _
  Sheets(1).Cells(i + RowNum, 39) = (1 - x) * ADS4MDot * 60 / DVIRho * 7.4805
  Sheets(1).Cells(i + RowNum, 40) = RXPress / 144 - ((IRWSTZ / 12 * DVIRho) / 144 - (RXz / 12 * DVIRho) / 144)
  Sheets(1).Cells(i + RowNum, 42) = ADS4v
  If Update > 25 Then
    Update = 0
    Calculate
  End If
'Determine Termination
  If zSat * 12 < Terminal Then
    i = MaxIter
    Sheets(1).Cells(19, 6) = "Termination Achieved"
    Termination = 1
  End If
Loop
  If Termination = 0 Then Sheets(1).Cells(19, 6) = "Simulation Completed"
  Sheets(1).Cells(19, 2) = Time
  Calculate
  Sheets(1).Cells(19, 5) = Time - StartTime
  Sheets(1).Activate
  With Application
    .Calculation = xlAutomatic
    .MaxChange = 0.001
  End With
End Sub

```

NOMENCLATURE

A	Area	Symbols	N	Total number of components
C_p	Specific heat for a constant pressure process		\vec{n}	Normal vector
C_v	Specific heat for a constant volume process		P	Pressure
D	Pipe inside diameter		Q	Heat
e	Total energy		q	Heat flux
f	Darcy friction factor		q'_{avg}	Average linear heat flux
g	Gravity		R	Rydbergs constant
h	Enthalpy		ρ	Density
h_L	Friction and form head loss		T	Temperature
k	Dimensionless friction coefficient		t	Time
K	Dimensionless friction coefficient strictly for form losses		u	Internal energy
ℓ	Pipe length		V	Volume
L	Core length		v	Velocity
M	Mass		W_μ	Viscous work
\dot{m}	Mass flow rate		W_s	Shaft work
			x	Vapor quality
			z	Elevation
		Subscripts		
ADS4	Pertaining to parameters involved with the ADS 4 line.		j	Integer index for the nodes in the core region.
break	Pertaining to parameters involved with the break.		IRWST	Pertaining to parameters involved with the IRWST.
bundle	Pertaining to parameters involved with the reactor bundle in the core.		node	Pertaining to parameters involved with the nodes in the core region.
core	Pertaining to parameters involved with the core.		RX	Pertaining to parameters involved with the reactor
DVI	Pertaining to parameters involved with the DVI.		rel	Pertaining to parameters involved with the relative diameter of the reactor..
f	Pertaining to parameters involved with liquid.		steam	Pertaining to parameters involved with the steam generated in the core.
g	Pertaining to parameters involved with water vapor.		sump	Pertaining to parameters involved with the sump.
i	Integer index for a time step.		tp	Pertaining to parameters involved with a two phase fluid.
inject	Pertaining to parameters involved with the injection fluid from the DVI lines.			
		Acronyms		
ACC	Accumulator			
ADS	Automatic Depressurization System			
AP600	Advance Plant 600 megawatt			
APEX	Advanced Plant EXperiment			
APOS	APEX Oscillation Simulator			
CMT	Core Makeup Tank			
DVI	Direct Vessel Injection			
IRWST	Incontainment Refueling Water Storage Tank			
PRHR	Primary Residual Heat Removal heat exchanger			
RS	Return to Saturation			
TOHL	Top Of Hot Leg			